U.S. ARMY COMBAT CAPABILITIES DEVELOPMENT COMMAND
CHEMICAL BIOLOGICAL CENTER

ABERDEEN PROVING GROUND, MD 21010-5424

DEVCOM CBC-TR-1799

Detecting Synthetic Opioids: Exploration of Surface-Enhanced Raman Spectroscopy and Development of Master Spectrum for Detection of Unknowns

Jason Guicheteau
Neal Kline
Phillip Wilcox
Ashish Tripathi
Erik Emmons
Andrew Walz
James Myslinski

RESEARCH AND OPERATIONS DIRECTORATE

April 2023

Disclaimer

The findings in this report are not to be construed as an official Department of the Army position unless so designated by other authorizing documents.

REPORT DOCUMENTATION PAGE

Form Approved
OMB No. 0704-0188

1. REPORT DATE *(DD-MM-YYYY)*	2. REPORT TYPE	3. DATES COVERED *(From - To)*
XX-04-2023	Final	Sep 2019–Jan 2022

4. TITLE AND SUBTITLE
Detecting Synthetic Opioids: Exploration of Surface-Enhanced Raman Spectroscopy and Development of Master Spectrum for Detection of Unknowns

5a. CONTRACT NUMBER
70RSAT19KPM000048

5b. GRANT NUMBER

5c. PROGRAM ELEMENT NUMBER

6. AUTHOR(S)
Guicheteau, Jason; Kline, Neal; Wilcox, Phillip; Tripathi, Ashish; Emmons, Erik; Walz, Andrew; and Myslinski, James

5d. PROJECT NUMBER

5e. TASK NUMBER

5f. WORK UNIT NUMBER

7. PERFORMING ORGANIZATION NAME(S) AND ADDRESS(ES)
Director, DEVCOM CBC, ATTN: FCDD-CBD-IS, APG, MD 21010-5424

8. PERFORMING ORGANIZATION REPORT NUMBER
DEVCOM CBC-TR-1799

9. SPONSORING / MONITORING AGENCY NAME(S) AND ADDRESS(ES)
U.S. Department of Homeland Security, Science and Technology Directorate; 2707 Martin Luther King Jr. Avenue, SE, Washington, DC 20528-0525

10. SPONSOR/MONITOR'S ACRONYM(S)
DHS S&T

11. SPONSOR/MONITOR'S REPORT NUMBER(S)

12. DISTRIBUTION / AVAILABILITY STATEMENT
Distribution Statement A. Approved for public release: distribution unlimited.

13. SUPPLEMENTARY NOTES

14. ABSTRACT: (Limit 200 words)
This effort, in support of the U.S. Department of Homeland Security, Science and Technology Directorate (Washington, DC), assessed the ability to augment current handheld Raman spectroscopic systems with surface-enhanced Raman spectroscopy substrates. The work was performed to understand pathways and analyze trace-level amounts of materials on contaminated surfaces. Additional work is reported on the construction of a unique single data element (library spectrum) that was developed with hundreds of synthetic opioid examples. The focus of this work was to assess whether the single spectrum could be used to detect the presence of an opioid even if the material was not in the system's database and had not been previously seen.

15. SUBJECT TERMS
Synthetic opioids
Surface-enhanced Raman spectroscopy (SERS)
Algorithm improvements
Sensor development

16. SECURITY CLASSIFICATION OF:			17. LIMITATION OF ABSTRACT	18. NUMBER OF PAGES	19a. NAME OF RESPONSIBLE PERSON
a. REPORT	b. ABSTRACT	c. THIS PAGE			Renu B. Rastogi
U	U	U	UU	50	19b. TELEPHONE NUMBER *(include area code)* (410) 436-7545

Blank

PREFACE

The work described in this report was authorized under project number 70RSAT19KPM000048. This work was started in September 2019 and completed in January 2022.

The use of either trade or manufacturers' names in this report does not constitute an official endorsement of any commercial products. This report may not be cited for purposes of advertisement.

This report has been approved for public release.

Acknowledgment

The authors acknowledge Dr. Rosanna Anderson (Department of Homeland Security, Science and Technology Directorate; Washington, DC) and her team for their support, guidance, and discussions throughout the program.

Blank

CONTENTS

FIGURES

TABLES

DETECTING SYNTHETIC OPIOIDS: EXPLORATION OF SURFACE-ENHANCED RAMAN SPECTROSCOPY AND DEVELOPMENT OF MASTER SPECTRUM FOR DETECTION OF UNKNOWNS

1. INTRODUCTION

Fentanyl is a powerful synthetic opioid that has fueled the ongoing opioid crisis worldwide. Recently in the United States, the number of deaths caused by synthetic opioids has increased by nearly 600%, from 5,444 in 2014 to 31,335 in 2018 (*1*). Similarly, reporting from U.S. forensic laboratories has documented 100,378 fentanyl samples in 2018 as compared to 5,541 fentanyl samples in 2014 (*1*). The numerous chemical analogs of synthetic opioids and the variety of purity levels encountered by civilian law enforcement, investigators, and defense users constantly challenge detection systems to be versatile in order to detect the threat. The Opioid Detection Program of the U.S. Department of Homeland Security, Science and Technology Directorate (Washington, DC) is sponsored the U.S. Army Combat Capabilities Development Command Chemical Biological Center (DEVCOM CBC; Aberdeen Proving Ground, MD) to further explore novel detection methodologies and determine whether newly developed techniques can be used to counteract the constantly changing landscape of synthetic opioid detection and transition bulk detectors to trace-level analysis systems.

To support this goal, two main research paths were followed: exploration of the augmentation of current Raman spectroscopic-based systems, which use enhanced Raman techniques to allow for trace analysis, and determination of whether a single uniquely constructed data element (a library spectrum) could be used to detect the presence of an opioid, even if the material had not been previously seen and was not in the system's database.

2. BACKGROUND

2.1 Surface-Enhanced Raman Spectroscopy

Portable Raman spectroscopy is a powerful tool for first responders and defense agencies for detection of bulk levels of threat materials in quantities greater than milligrams and milliliters. Raman is the inelastic scattering of photons by molecules. The scattered photons form sharp-lined spectral features that can be matched to a library to detect a threat, even in the presence of complex backgrounds. However, two main drawbacks to Raman are that the inelastic scattering process is relatively weak, and fluorescence can hinder the Raman return and render a detection almost impossible. Over the past decade, industry has made strides in mitigating both issues. Wavelengths have been shifted further into the near-infrared or deep-ultraviolet portions of the electromagnetic spectrum to suppress the fluorescence with variable success. More recently, work has moved toward use of surface-enhanced Raman spectroscopy (SERS) to overcome the weak return.

When SERS is used, nanometallic substrates locally amplify electromagnetic fields at or near particle surfaces, which can provide a signal enhancement factor of 106 as compared to normal Raman spectroscopy. Figure 1 shows this pictorially with thiophenol (TP)

molecules adsorbing onto a gold surface and exhibiting electronic enhancement upon irradiation with a laser. The normal Raman spectrum at 1×10^{-4} M exhibits no visual peaks for detection; however, the SERS spectrum at the same concentration shows a multitude of peaks that produce the characteristic chemical fingerprint that can be used for library matching.

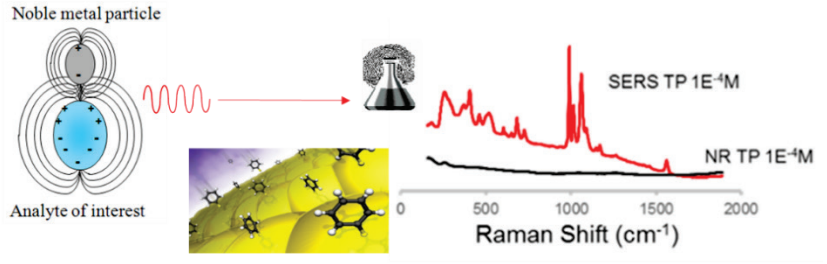

Figure 1. SERS scheme of TP adsorbing onto a gold nanostructure to yield an enhanced Raman signal. SERS TP, SERS spectrum; NR TP, normal Raman spectrum.

Furthermore, the SERS process quenches the majority of fluorescence, which (as mentioned above) can hinder normal Raman measurements. Given these two advantages, along with decreased integration times and reduced laser power requirements for analysis, SERS is positioned to be an ideal technique for trace-level (microgram or less), low-consumable detection schemes. Despite these advantages, the successful transition from research laboratories to real-world applications has been very limited. However, industry has recently started developing SERS-based kits and accessories to augment portable Raman systems in an attempt to push SERS into the field for trace-level and mixture analysis of materials, specifically, synthetic opioids, narcotics, and explosives. In this research effort, we examined these newly available SERS kits and accessories using small research-grade spectrometers, prototype systems, and commercially available portable Raman sensors.

2.2 SERS Substrates

For this work, we concentrated on two commercially available SERS kits associated with portable Raman systems: Raman printed SERS (P-SERS) strips (Metrohm USA; Riverview, FL) and H-Kits (Thermo Scientific; Waltham, MA).

The P-SERS strips (Figure 2A) were designed to be used with the Metrohm Instant Raman Analyzer (MIRA) DS system. The SERS-active area is made up of silver or gold colloids (nanoparticles) that have been deposited onto a paper-based test strip in a 1 × 1 cm area, and the strip is then placed under varying magnifications of scanning electron microscopy (SEM). The H-Kit (Figure 2B) is designed to work with the Gemini Raman system (Thermo Scientific). The H-Kit stick contains a SERS active surface, which is an approximately 2 × 2 mm silicon wafer with gold nanoparticles structured in pillar arrangements over its entire active area. The wafer is then placed under various SEM magnifications.

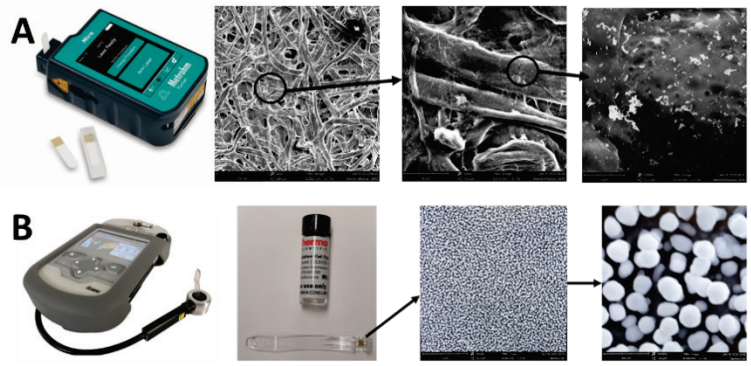

Figure 2. (A) Metrohm P-SERS strips showing metallic nanoparticles imbedded in fibrous backing materials. (B) Thermo H-Kit substrate of metallic nanoparticle pillar structures on a silicon background.

The SERS substrates are associated with the two commercial instruments; however, our goal was not only to examine SERS instrument efficiency. We also sought to identify the various optimization parameters for acquiring SERS signatures and to determine whether the SERS substrates could be used with different instruments (aside from their commercial pairings). To that end, in the research detailed herein, additional Raman instrumentation was used to compare and contrast SERS responses from the substrates, with a focus on identifying detection performance against a range of synthetic opioids. This work is detailed in Section 3.1.

2.3 Detecting the Unknown

The chemical structure of fentanyl (Figure 3) consists of four main components: an aniline ring (cyan), a piperidine ring (purple), an *N*-propionyl group (green), and a phenethyl group (red). The replacement or substitution of any of these functional groups creates fentanyl analogs of varying toxicity. Worldwide crackdown on specific precursors can cause trafficking organizations to shift to other synthetic routes or analogs. The U.S. Drug Enforcement Agency (DEA; Arlington, VA) explicitly schedules 46 different fentanyl compounds but has a catch-all schedule for any "fentanyl-related substances, their isomers, esters, ethers, salts and salts of isomers, esters and ethers" (*2*). This broad definition poses a challenge for the development of Raman detection instruments, which work by comparing collected spectra to an internal library. As new analogs emerge and gain prominence, it is not always feasible, cost-effective, or timely to acquire a sample of the new compound, add a new element to the library, and disseminate the new library to operators in the field. Instead, it is preferable to have a screening method capable of classifying unknown fentanyl analogs while minimizing false alarms on other benign unknown substances. In Section 4, we explore the possibility of creating a unique, singular, synthetic opioid spectrum in order to demonstrate the classification of spectra as fentanyl or non-fentanyl, even if the actual target does not exist in a library database.

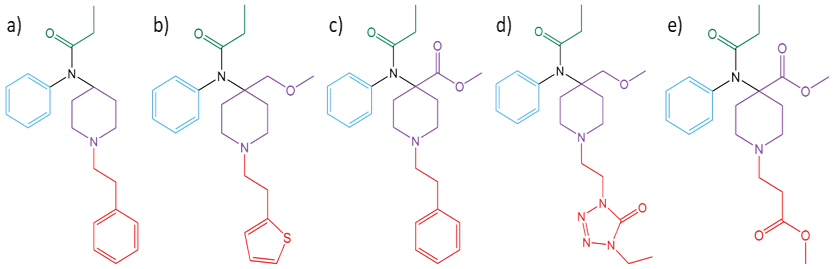

Figure 3. Chemical structures for (a) fentanyl, (b) sufentanil, (c) carfentanil, (d) alfentanil, and (e) remifentanil. Other fentanyl analogs can be created by altering the phenethyl group (red), the piperidine ring (purple), the aniline ring (cyan), or the *N*-propionyl group (green).

3. SURFACE-ENHANCED RAMAN OF OPIOIDS

3.1 Experimental Section

3.1.1 Chemicals and Materials

Five fentanyl compounds were analyzed in this study: fentanyl hydrochloride, sufentanil citrate, alfentanil hydrochloride, benzylfentanyl hydrochloride, and remifentanil hydrochloride. All are regulated as Schedule II by the DEA except for benzylfentanyl, which is a DEA Schedule I chemical. The fentanyl hydrochloride was purchased from Sigma-Aldrich (St. Louis, MO). Purity was 94%, as verified using liquid chromatography–mass spectrometry (LC–MS). The other four compounds were synthesized by the DEVCOM CBC Agent Chemistry Branch. Purities for these compounds were all 98% or higher, as measured using nuclear magnetic resonance (NMR) and LC–MS. Stock solutions were made for fentanyl hydrochloride (2.4×10^{-2} M), sufentanil (10×10^{-2} M), alfentanil (1.6×10^{-2} M), benzylfentanyl (10×10^{-2} M), and remifentanil (2.4×10^{-2} M). Sufentanil and alfentanil stock solutions had to be made with an 80/20 water/ethanol (EtOH) mixture so that the compounds would dissolve completely. Each prepared stock solution was then serially diluted to obtain solutions of 1.0×10^{-2}, 1.0×10^{-3}, 1.0×10^{-4}, 1.0×10^{-5}, 1.0×10^{-6}, 1.0×10^{-7}, 1.0×10^{-8}, and 1.0×10^{-9} M.

3.1.2 Raman Measurements

Raman measurements were performed with a tabletop Raman setup and a commercial handheld Raman instrument. The tabletop setup consisted of a 785 nm RP-785 Raman probe (Innovative Photonic Solutions [IPS]; Plainsboro, NJ), a 785 nm IPS multi-mode digital M-Type module power source (model no. 10785MM0350MF), and a Wasatch Photonics (Logan, UT) Raman 785 ER spectrometer operating at 10 °C with a 10 µm slit opening to obtain a spectral resolution of approximately 6 cm^{-1}; no collection optics were used. An IPS Raman probe was used to obtain normal Raman measurements through glass vials (Sigma-Aldrich; product no. V7130) that contained prepared stock and serially diluted fentanyl samples. The probe was situated horizontally on a laser table, and the glass vial containing sample solution was placed in front of the probe for data collection. The optimal measurement distance was

determined by manually adjusting the sample distance from the probe to optimize the signal-to-noise ratio (SNR). Normal Raman data were collected with a laser power of 0.337 W, a 5 s integration time, and five co-added spectra for each sample solution measured. A background trace was acquired with water in a glass scintillation vial for remifentanil, benzylfentanyl, and fentanyl; for alfentanil and sufentanil, the background was an 80/20 water/EtOH mixture. Each background subtraction was a point-to-point subtraction of the background trace from the spectral data for the fentanyl compound.

The commercial handheld instrument was the MIRA DS system operating at 785 nm with a spectral resolution of 8–10 cm^{-1}. The MIRA intelligent universal attachment (IUA) operating in position 2 was used for normal Raman measurements that were made through glass vials of prepared stock and serially diluted fentanyl samples. Optimal measurement distance was determined by manually adjusting the distance between the sample and the IUA to optimize the SNR. The IUA is a three-position collection optics accessory that allows the focal length of the MIRA to be changed to interrogate surfaces, bags, or bottles. The MIRA DS system was situated horizontally on the laser table, and a glass vial containing sample solution was placed in front of the IUA for data collection. Normal Raman data were collected with a laser power of setting of 5 (50 mW), a 5 s integration time, a no-raster setting, and five co-added spectra for each sample solution measured. Background collection and subtraction were performed using the same procedure as for the tabletop Raman setup.

3.1.3 SERS Measurements

SERS measurements were acquired with silver (Ag) and gold (Au) P-SERS substrates that were purchased from Metrohm. P-SERS strips were prepared by pipetting a 10 µL droplet onto the active area of the strip or by immersing the strip in approximately 0.5 mL of fentanyl sample solution for 1, 5, or 10 min. On the tabletop Raman setup (the Wasatch spectrometer), measurements were made by situating the IPS Raman probe vertically, placing the strip on an adjustable vertical stage, and adjusting the stage until the optimal SNR was obtained (Figure 4A). Spectra were collected using a 32.0 mW laser power setting, a 1.4 s integration time, five co-added spectra, and no collection optics. Background traces were acquired for the droplet and soaking experiments by pipetting a 10 µL droplet of water onto the active area of the P-SERS strip or by immersing the P-SERS strip in water for 1, 5, or 10 min and then obtaining background measurements after the P-SERS strip was prepared. Each background subtraction was a point-to-point subtraction of the background trace from the spectral data for the fentanyl compound.

After the initial measurements were performed on the Wasatch spectrometer, additional P-SERS strips were similarly prepared and analyzed on the MIRA DS system using the SERS optical attachment (Figure 4B). Spectra were collected by placing prepared P-SERS strips into the SERS attachment and using a laser power setting of 5 (50 mW), a 3 s integration time, and three co-added spectra. Two sets of experiments were performed using P-SERS strips under these conditions with laser rastering turned on and off. The same procedures that were used for the tabletop Raman setup were also used for background collection and subtraction.

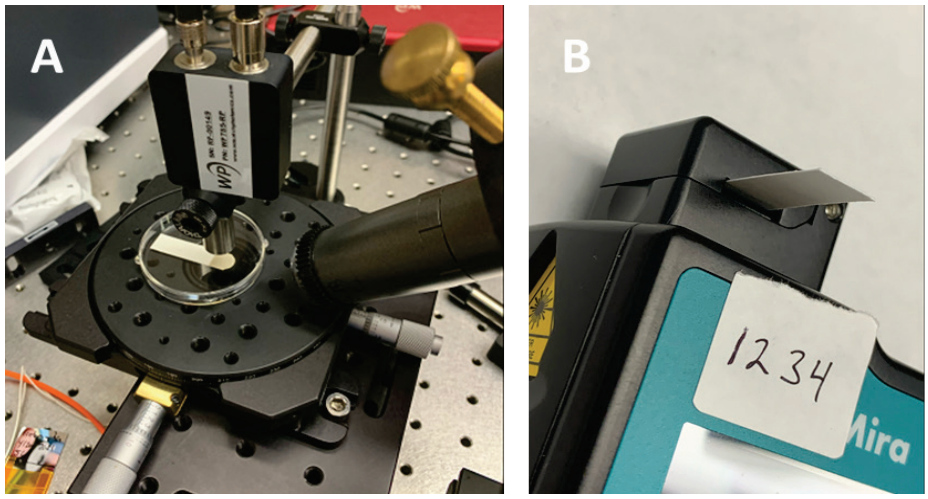

Figure 4. (A) Wasatch Raman 785 ER spectrometer and probe set up for SERS analysis; and (B) Metrohm MIRA SERS optical attachment with P-SERS strip.

3.2 Results and Discussion: P-SERS Strips

3.2.1 Normal Raman Measurements

Figure 5 shows the normal Raman spectra for the five fentanyl compounds (with backgrounds subtracted) that were collected using the tabletop Raman setup (Wasatch). In the sufentanil and alfentanil traces (Figures 5D and 5E, respectively), EtOH overwhelmed the normal Raman spectra, as shown by the prominent EtOH peaks near 1040 and 1460 cm^{-1}. This made background subtraction difficult because large negative-subtraction features remained after data processing was completed for those solutions, although several features of alfentanil are present in the 1.00×10^{-2} spectrum at 721, 795, and 1460 cm^{-1}. Spectral features for benzylfentanyl, fentanyl, and remifentanil are easily identifiable (Figure 5; A, B, and C, respectively), and it appears that a normal Raman response was not observed for any of the fentanyl compounds at the 1.00×10^{-4} M concentration level.

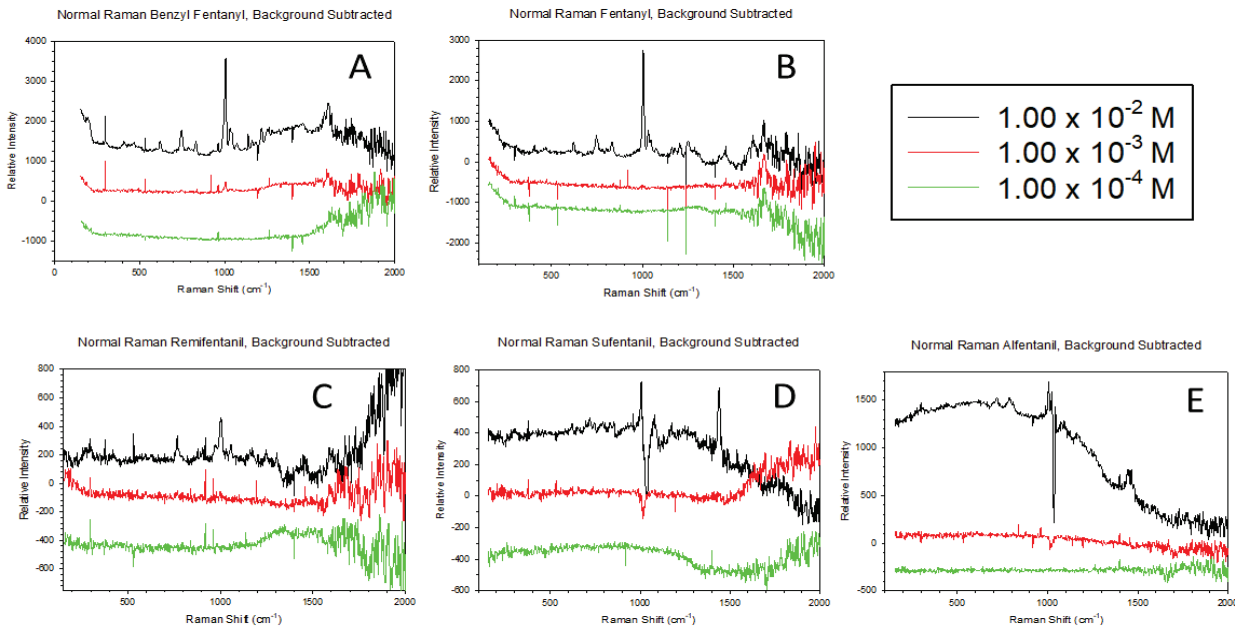

Figure 5. Normal Raman spectra obtained using the tabletop system with fentanyl analogs (background traces subtracted): (A) benzylfentanyl, (B) fentanyl, (C) remifentanil, (D) sufentanil, and (E) alfentanil.

Figure 6 shows the normal Raman spectra for the five fentanyl compounds (with backgrounds subtracted) that were collected with the MIRA DS Advanced system. As occurred when the tabletop Raman setup was used, the spectra for sufentanil and alfentanil (Figure 6; D and E, respectively) were overwhelmed by EtOH Raman signatures. Although alfentanil signatures were observed in the subtracted trace that was obtained using the tabletop Raman setup (Figure 5E), no alfentanil signatures could be observed (Figure 6E) from spectra obtained using the MIRA system. This was most likely due to the difference in laser power that was used in the experiments: 0.337 W was used in the tabletop Raman setup, whereas 50 mW was used with the MIRA system. These were the maximum power settings for each system. Spectral features for benzylfentanyl, fentanyl, and remifentanil (Figure 6; A, B, and C, respectively) were observed in the Raman spectra of the stock solutions for each compound but were not observed in the 1.00×10^{-3} M diluted solutions.

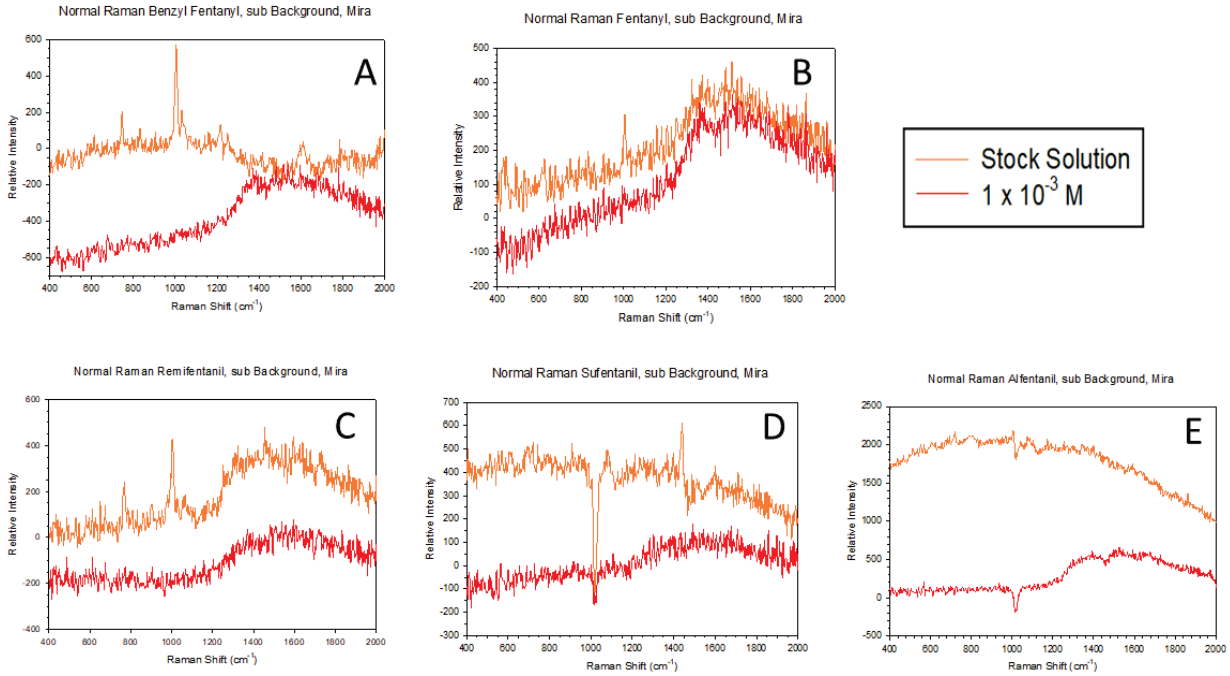

Figure 6. Normal Raman spectra obtained using the MIRA DS Advanced system with fentanyl analogs (background traces subtracted): (A) benzylfentanyl, (B) fentanyl, (C) remifentanil, (D) sufentanil, and (E) alfentanil.

3.2.2 Tabletop Raman SERS Droplet Protocol

Figures 7–11 show the results of the droplet Ag and Au P-SERS experiments on the different fentanyl compounds obtained using the tabletop Raman setup (Wasatch spectrometer). The backgrounds observed for the Ag and Au P-SERS strips were substantially different: the Au background was much more complicated and contained many features as compared to the relatively broad, featureless background of the Ag strips. The more complicated background for the Au strips led to a more difficult subtraction, and more negative subtraction features were observed than were identified for the Ag strips.

The SERS spectra of the Ag and Au strips were fairly consistent in terms of observed spectral features for fentanyl, benzylfentanyl, and remifentanil (Figures 8–10, respectively). For alfentanil and sufentanil (Figures 7 and 11, respectively), substantial differences in spectral features existed between the Ag and Au strips. This was thought to be caused by the analyte binding differently to the Ag or Au surface, which would result in different vibrational modes being SERS enhanced.

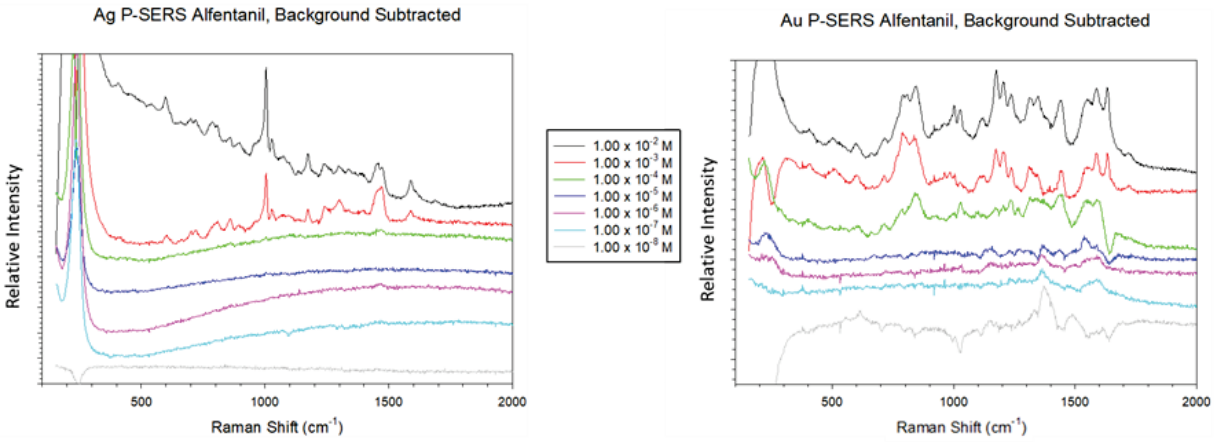

Figure 7. Alfentanil Ag (left) and Au (right) P-SERS droplet experiment spectra.

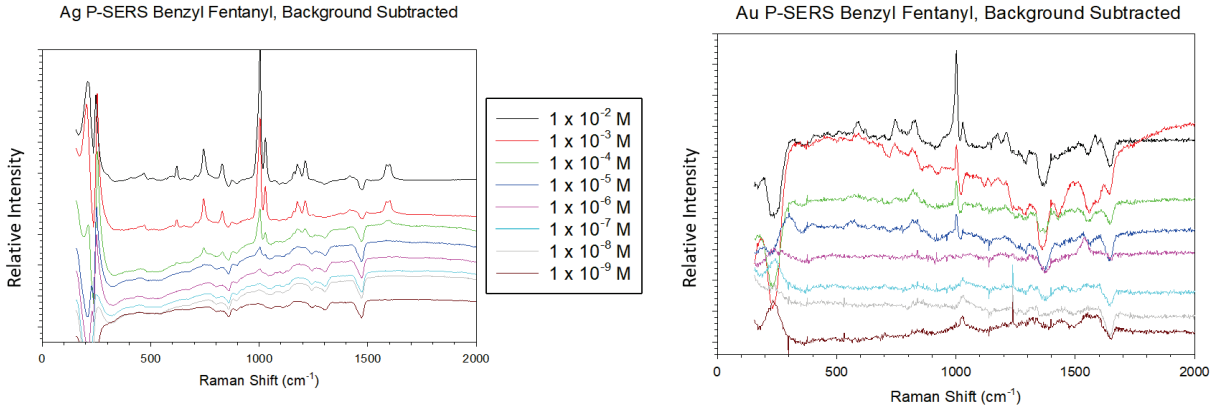

Figure 8. Benzylfentanyl Ag (left) and Au (right) P-SERS droplet experiment spectra.

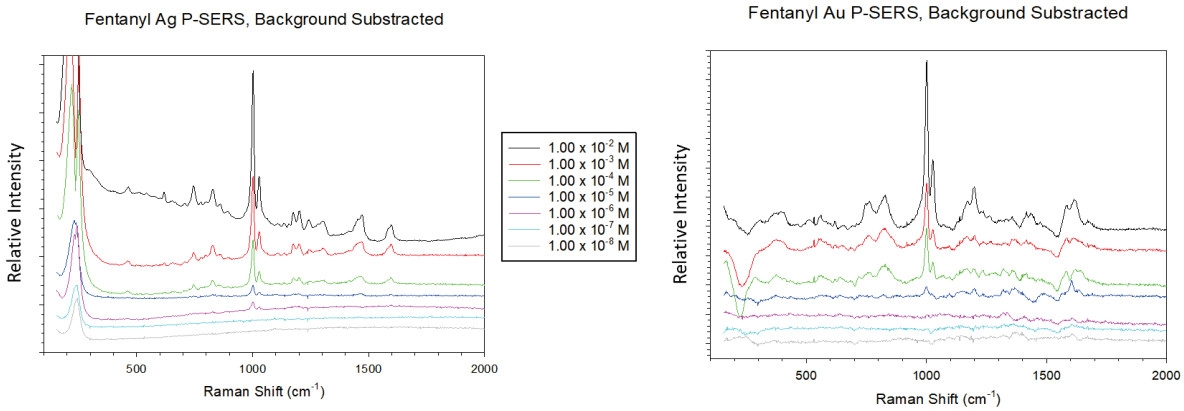

Figure 9. Fentanyl Ag (left) and Au (right) P-SERS droplet experiment spectra.

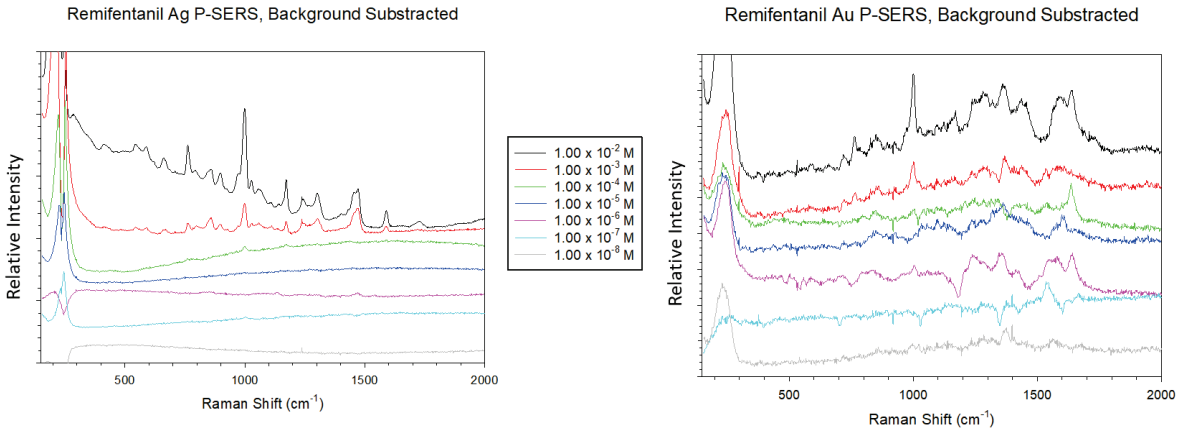

Figure 10. Remifentanil Ag (left) and Au (right) P-SERS droplet experiment spectra.

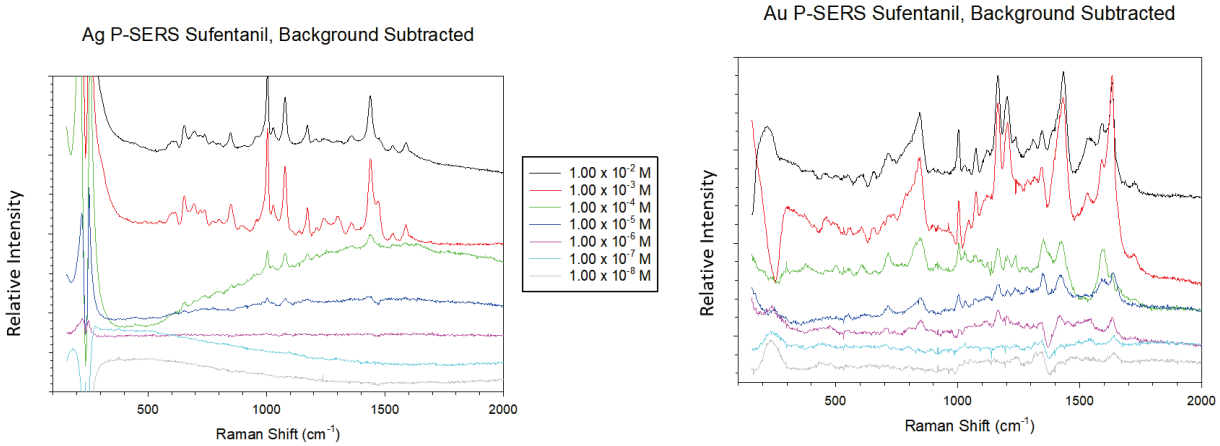

Figure 11. Sufentanil Ag (left) and Au (right) P-SERS droplet experiment spectra.

Table 1 summarizes the limits of detection (LODs) observed for the Ag and Au P-SERS strips with use of the tabletop Raman system and the droplet protocol. The Ag strips performed better overall with one exception: sufentanil was observed to have a lower LOD with the Au strips instead of the Ag. It was somewhat expected that the LODs would be lower for the Ag substrates, given that typically, Ag is more sensitive than Au in the SERS capacity; however, Ag can suffer from oxidation instability, which can affect overall shelf life. A shelf-life study was not performed as part of this research to demonstrate this. Metrohm Raman representatives stated that the Ag strips should be stable for approximately 6–12 months when they are stored in proper conditions (with the supplied packaging maintained).

Table 1. LODs for Fentanyl Compounds Obtained Using Ag and Au P-SERS Strips: Droplet Experiments

Fentanyl Compound	LOD (M)	
	Ag P-SERS Droplet	Au P-SERS Droplet
Sufentanil	1.00×10^{-5}	1.00×10^{-6}
Alfentanil	1.00×10^{-4}	1.00×10^{-4}
Fentanyl	1.00×10^{-6}	1.00×10^{-5}
Benzylfentanyl	1.00×10^{-6}	1.00×10^{-5}
Remifentanil	1.00×10^{-4}	1.00×10^{-3}

3.2.3 Handheld MIRA SERS with Droplet Protocol

Figures 12–16 show the results of the droplet Ag P-SERS experiments for the various fentanyl compounds obtained using the Raman MIRA DS Advanced handheld spectrometer. After comparing the performance results for the Ag and Au strips (in Section 3.2.2), we decided to continue experiments with only the Ag strips, given their superior performance and the background issues associated with the Au strips. Two sets of experiments, one under laser raster conditions (in which the beam vibrates in a figure-eight pattern to minimize the power onto the sample and increase the area of interrogation) and the other under no-raster conditions (in which the beam is held steady) were completed. The laser raster setting consistently outperformed the no-raster setting, apart from a few exceptions at the highest concentrations measured (1.00×10^{-3} M) for sufentanil and benzylfentanyl, where the no-raster setting performed better.

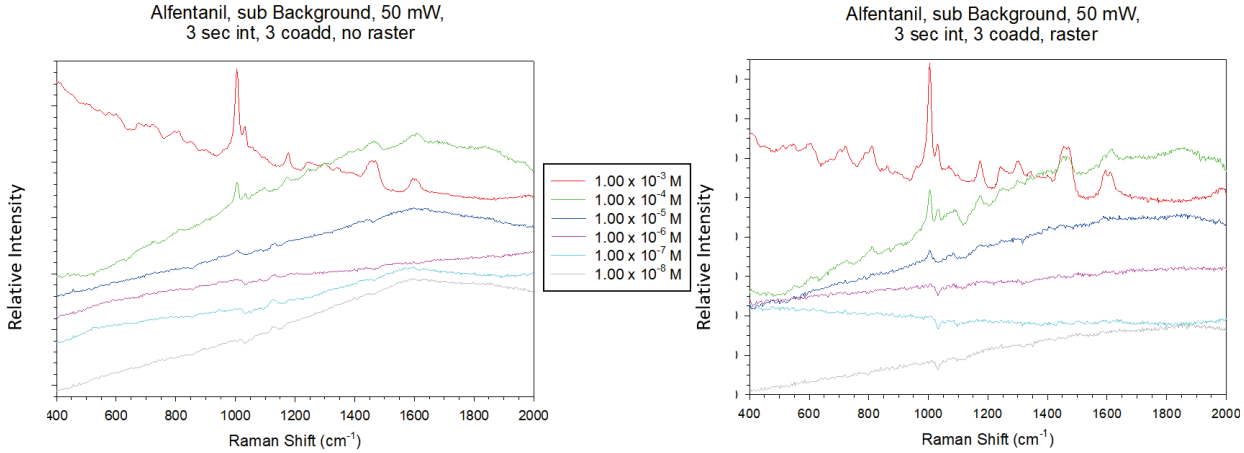

Figure 12. Alfentanil Ag P-SERS droplet summary comparing SERS spectra obtained with no-raster (left) and laser raster (right) instrument settings.

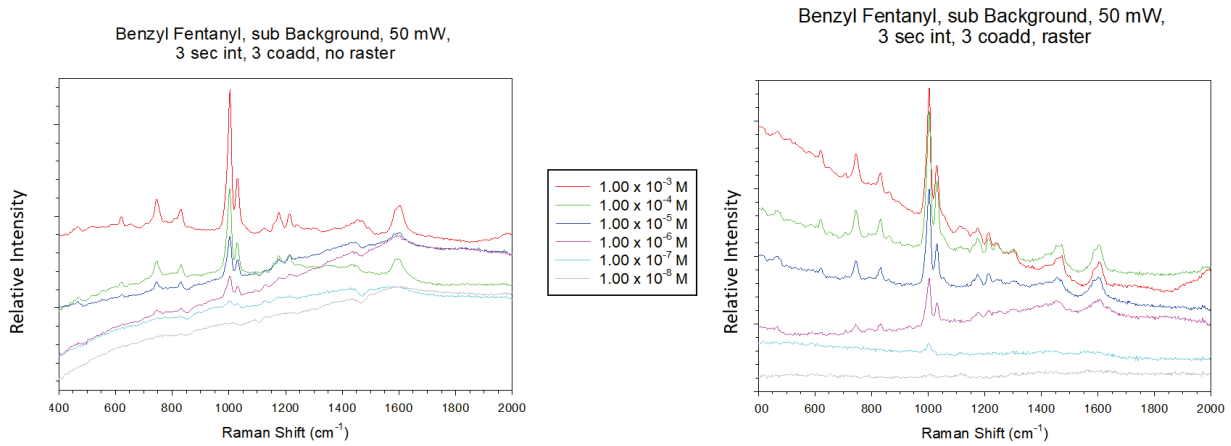

Figure 13. Benzylfentanyl Ag P-SERS droplet summary comparing SERS spectra obtained with no-raster (left) and laser raster (right) instrument settings.

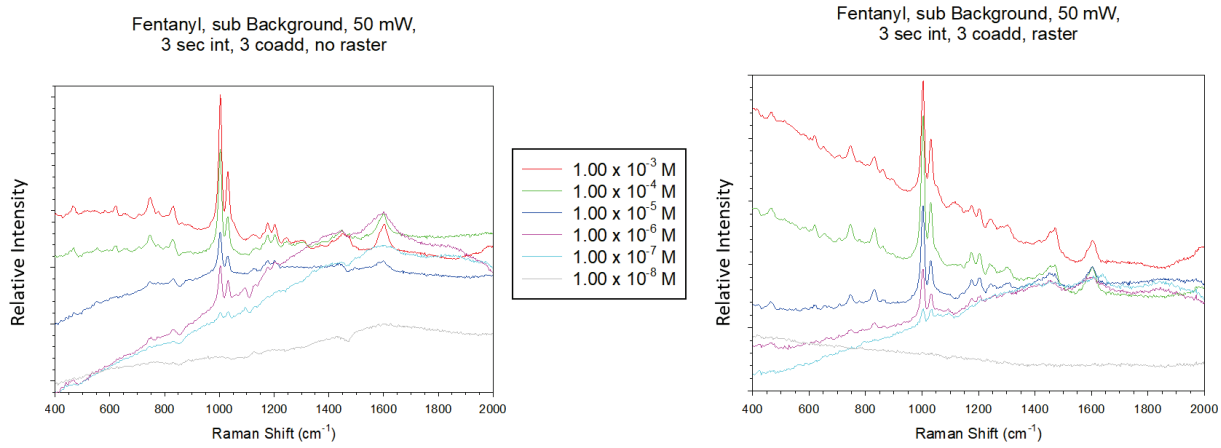

Figure 14. Fentanyl Ag P-SERS droplet summary comparing SERS spectra obtained with no-raster (left) and laser raster (right) instrument settings.

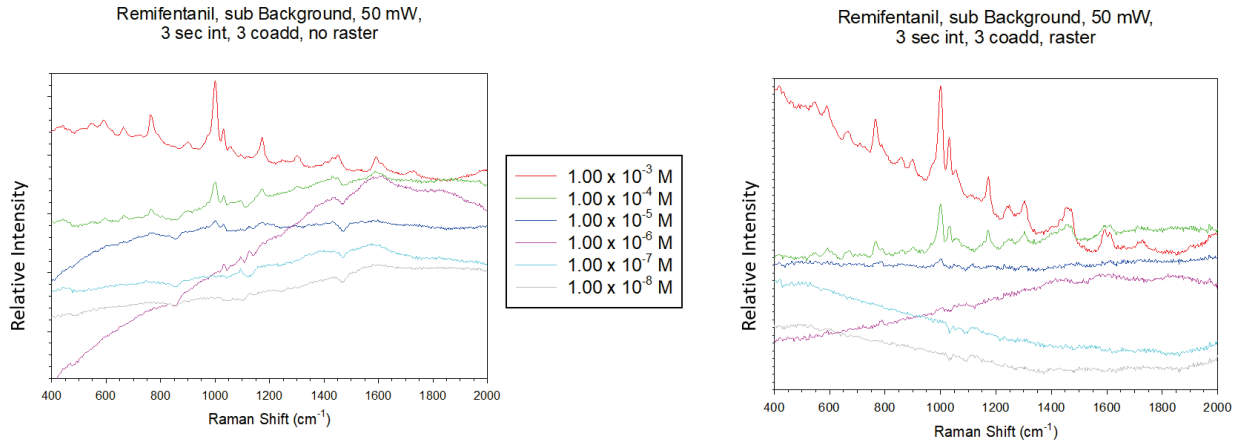

Figure 15. Remifentanil Ag P-SERS droplet summary comparing SERS spectra obtained with no-raster (left) and laser raster (right) instrument settings.

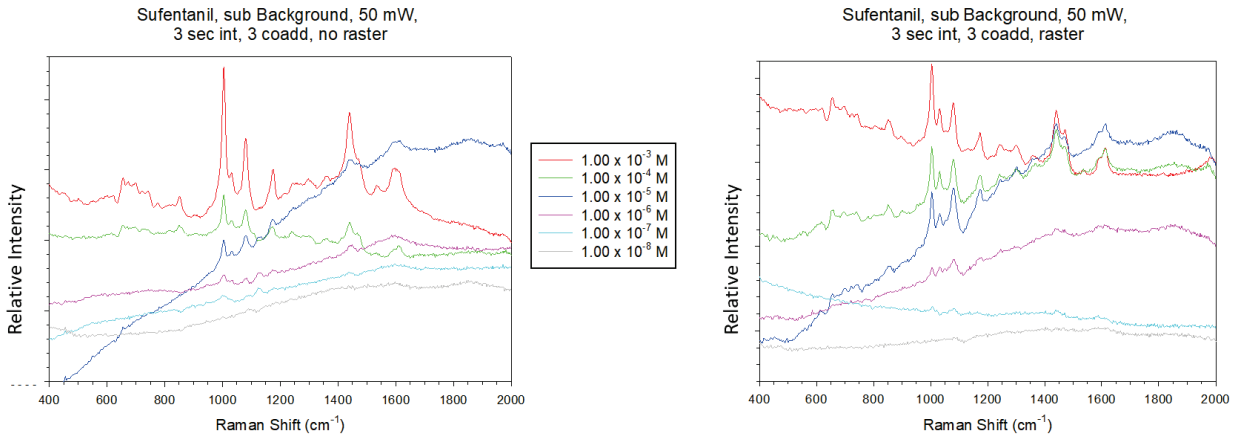

Figure 16. Sufentanil Ag P-SERS droplet summary comparing SERS spectra obtained with no-raster (left) and laser raster (right) instrument settings.

Table 2 summarizes the LODs observed using the droplet protocol for the MIRA DS Advanced system under raster and no-raster conditions. The laser raster setting performed better overall and provided lower LODs and better SNRs for spectral data obtained at lower concentrations.

Table 2. LODs for Fentanyl Compounds Obtained Using MIRA DS System Under Raster and No-Raster Conditions

Fentanyl Compound	LOD for Ag P-SERS Droplet with MIRA DS System (M)	
	Raster	No Raster
Sufentanil	1.00×10^{-6}	1.00×10^{-5}
Alfentanil	1.00×10^{-5}	1.00×10^{-4}
Fentanyl	1.00×10^{-7}	1.00×10^{-6}
Benzylfentanyl	1.00×10^{-7}	1.00×10^{-6}
Remifentanil	1.00×10^{-4}	1.00×10^{-4}

3.2.4 Wasatch Tabletop Raman SERS with Soaking Protocol

After completion of the initial droplet experiments, in which we followed the vendor's guidelines and suggestions for best use of the substrates, we performed soaking experiments. The purpose of these experiments was to determine whether allowing more time for the target analyte to interact with the surface would improve the LODs.

Figures 17–21 show the results of the Ag P-SERS soaking experiments for the different fentanyl compounds with use of the tabletop Raman setup. Background-subtracted spectra were presented at immersion times of 1, 5, and 10 min. When the soaking data were compared with the droplet data, an improvement in SNR was observed for all three immersion times, and an increase in LOD (of about one order of magnitude) occurred across all of the fentanyls.

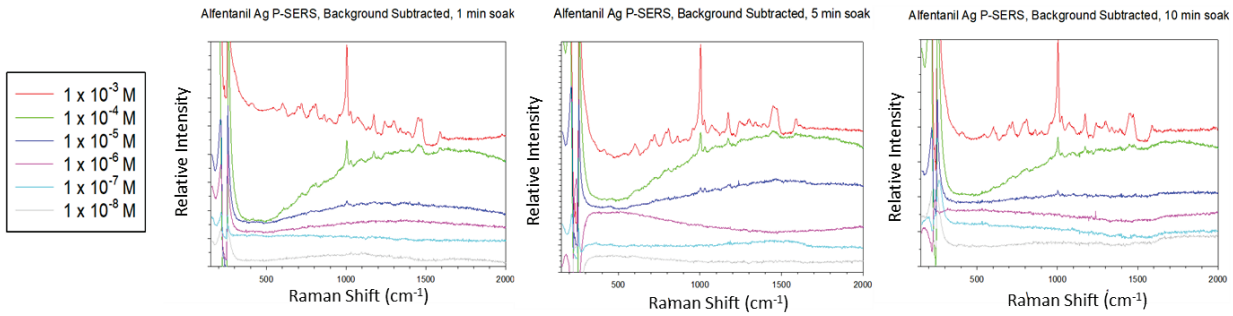

Figure 17. Alfentanil Ag P-SERS soaking experiments at 1, 5, and 10 min immersion times.

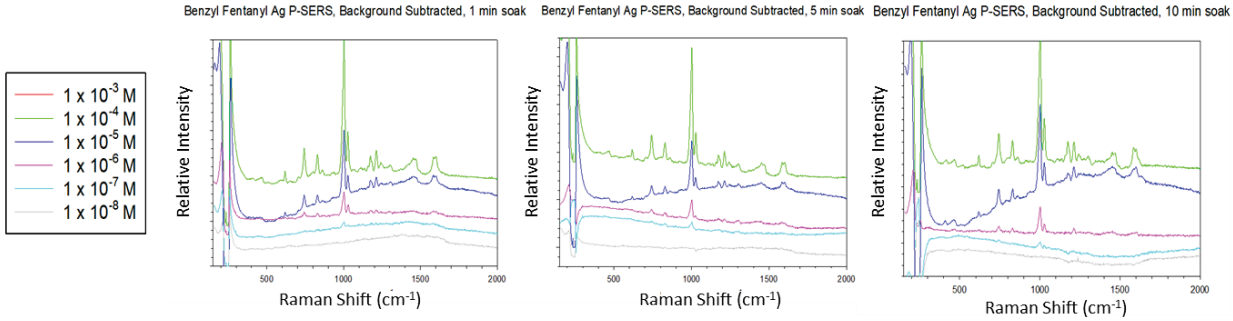

Figure 18. Benzylfentanyl Ag P-SERS soaking experiments at 1, 5, and 10 min immersion times.

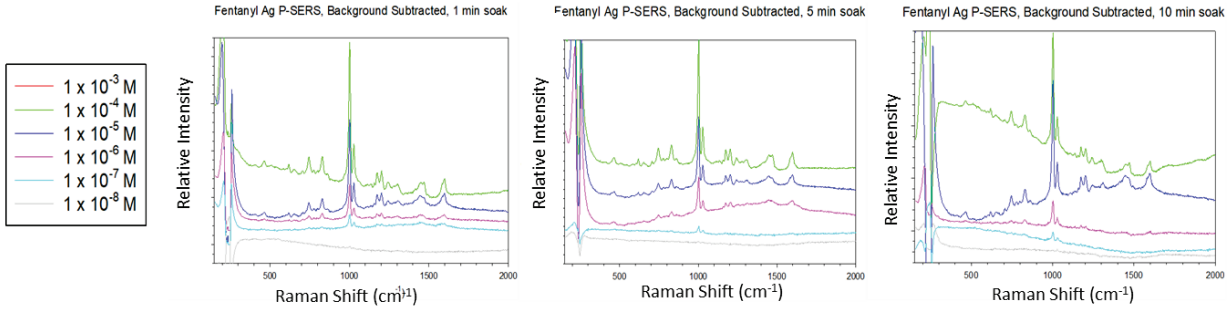

Figure 19. Fentanyl Ag P-SERS soaking experiments at 1, 5, and 10 min immersion times.

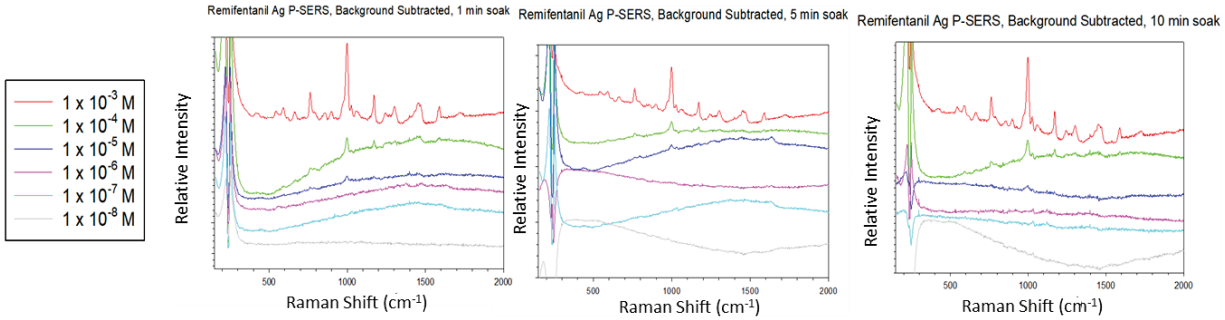

Figure 20. Remifentanil Ag P-SERS soaking experiments at 1, 5, and 10 min immersion times.

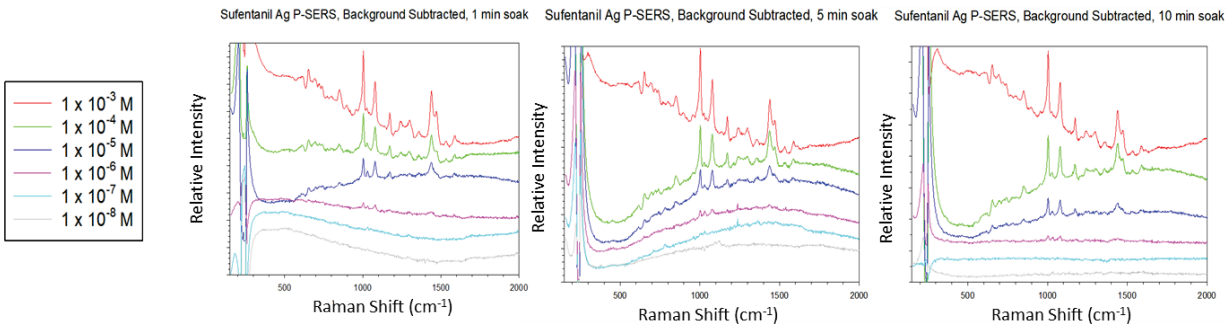

Figure 21. Sufentanil Ag P-SERS soaking experiments at 1, 5, and 10 min immersion times.

Table 3 shows the LODs that were observed for the different fentanyl compounds with use of the tabletop Raman system and the soaking protocol. The LODs and SNRs appear to be maximized at the 1 min immersion time, as no additional benefit was observed in the 5 and 10 min immersion times.

Table 3. LODs for Fentanyl Compounds Obtained Using Wasatch Tabletop Raman System with 1, 5, and 10 min Immersion Times

Fentanyl Compound	LOD (M)		
	Ag P-SERS 1 min Immersion	Ag P-SERS 5 min Immersion	Ag P-SERS 10 min Immersion
Sufentanil	1.00×10^{-6}	1.00×10^{-6}	1.00×10^{-6}
Alfentanil	1.00×10^{-5}	1.00×10^{-5}	1.00×10^{-5}
Fentanyl	1.00×10^{-7}	1.00×10^{-7}	1.00×10^{-7}
Benzylfentanyl	1.00×10^{-7}	1.00×10^{-7}	1.00×10^{-7}
Remifentanil	1.00×10^{-5}	1.00×10^{-5}	1.00×10^{-5}

3.2.5 MIRA Handheld Raman SERS with Soaking Protocol

Figures 22–26 show the Ag P-SERS experiments for the various fentanyl compounds with the use of the Raman MIRA DS Advanced handheld spectrometer and the 1 min soaking protocol. After the results reported in Section 3.2.4 were compared, only the 1 min immersion time was used with the MIRA DS system because additional time soaking did not provide any benefit. Two sets of experiments under laser raster and no-raster conditions were completed. Using the laser raster setting appeared to improve the spectral data acquired, but the improvement was not as pronounced as it was described in Section 3.2.3, when the raster and no-raster settings with the droplet protocol were compared.

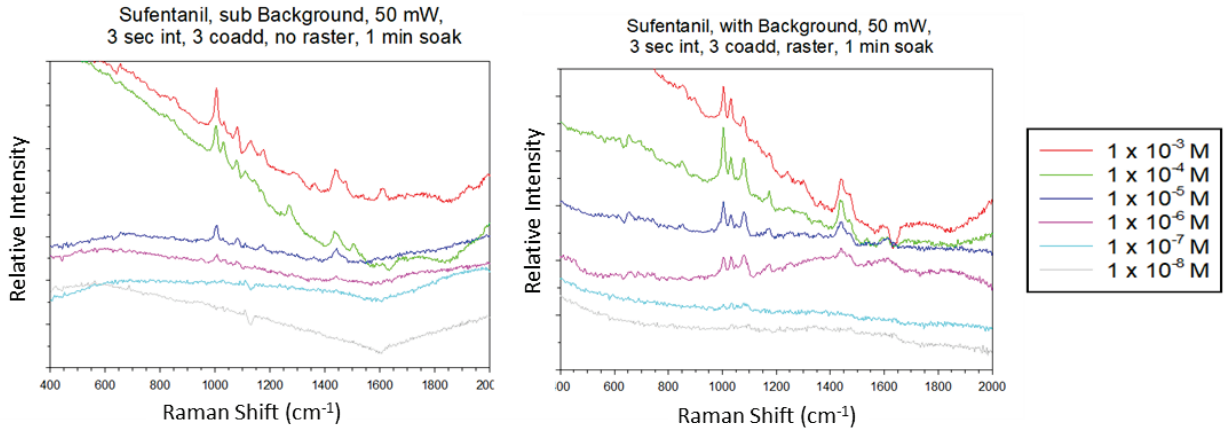

Figure 22. Sufentanil Ag P-SERS soaking experiment with MIRA DS at 1 min immersion time.

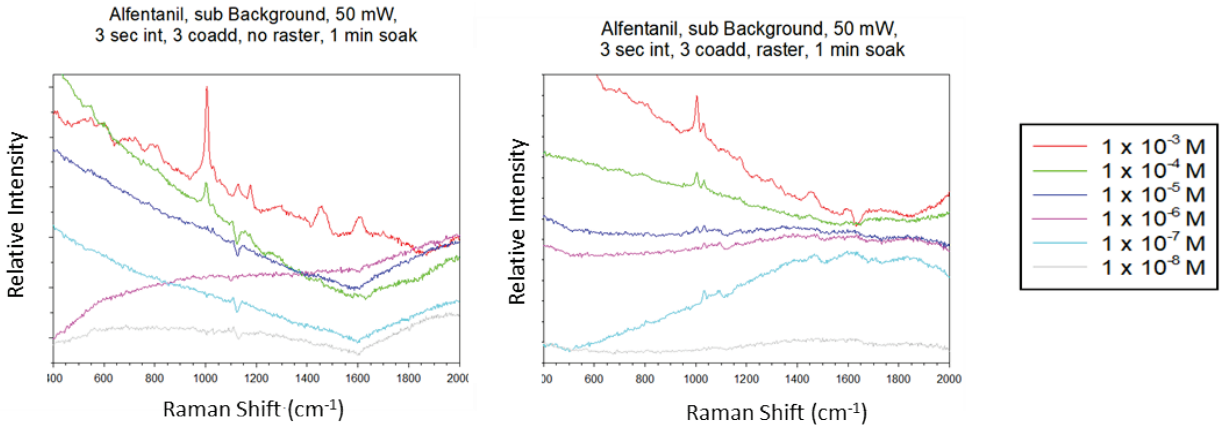

Figure 23. Alfentanil Ag P-SERS soaking experiment with MIRA DS at 1 min immersion time.

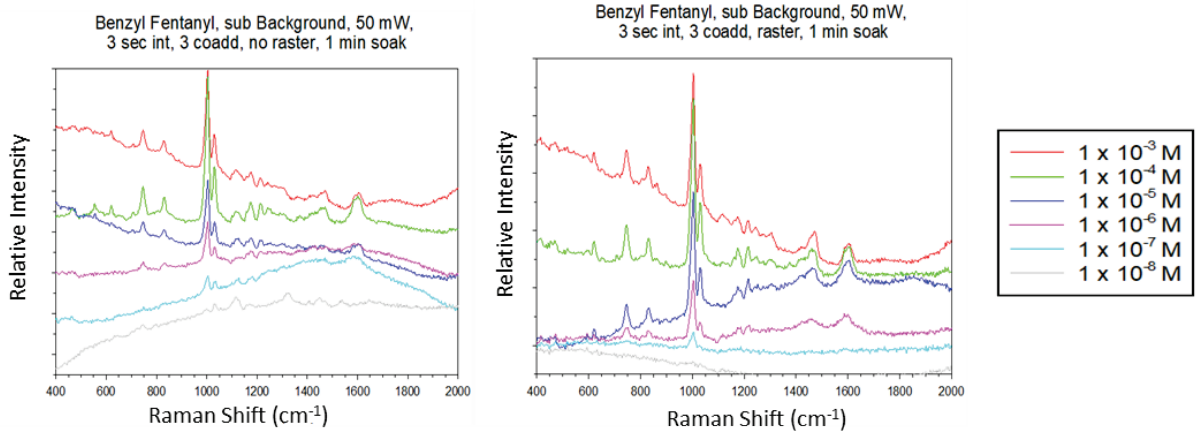

Figure 24. Benzylfentanyl Ag P-SERS soaking experiment with MIRA DS at 1 min immersion time.

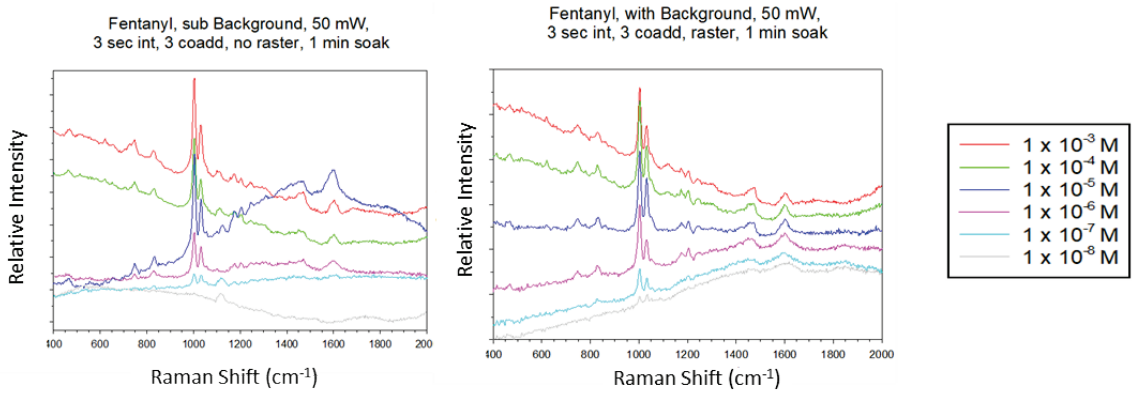

Figure 25. Fentanyl Ag P-SERS soaking experiment with MIRA DS at 1 min immersion time.

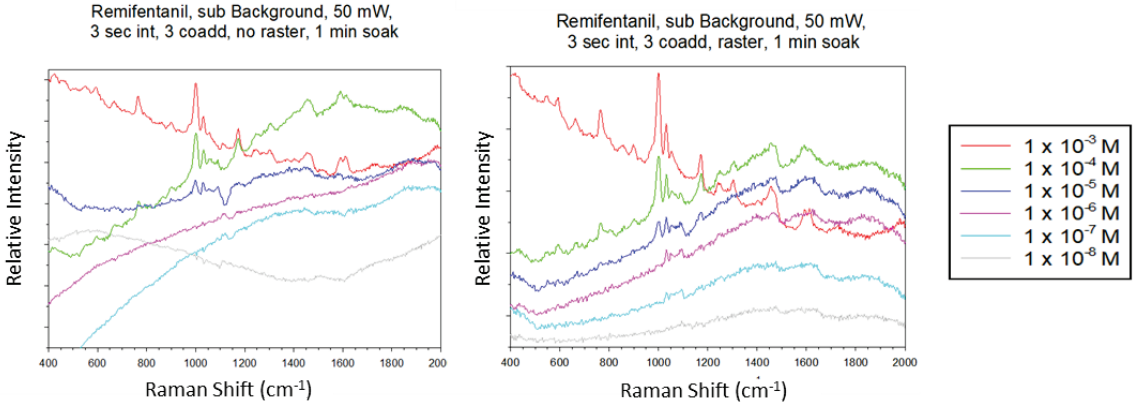

Figure 26. Remifentanil Ag P-SERS soaking experiment with MIRA DS at 1 min immersion time.

Table 4 summarizes the LODs that were observed with use of the handheld MIRA DS system under raster and no-raster conditions and the soaking protocol. The laser raster setting performed better overall and provided lower LODs and better SNRs for spectral data obtained at lower concentrations. This is explained by the rastering laser beam providing more opportunity for interaction between bound analyte and the Ag nanoparticles. Alternatively, under the no-raster condition, the beam remains stationary, and only information from that sole point contained within the beam diameter can be interrogated. This is an additional advantage associated with the MIRA DS system as compared to traditional handheld Raman systems, in which beams are typically stationary.

Table 4. LODs for Fentanyl Compounds Obtained Using Handheld MIRA DS System with 1 min Immersion Time

Fentanyl Compound	LOD (M)	
	MIRA DS No Raster	MIRA DS Raster
Sufentanil	1.00×10^{-6}	1.00×10^{-6}
Alfentanil	1.00×10^{-4}	1.00×10^{-5}
Fentanyl	1.00×10^{-7}	1.00×10^{-7}
Benzylfentanyl	1.00×10^{-7}	1.00×10^{-7}
Remifentanil	1.00×10^{-5}	1.00×10^{-5}

3.3 Summary: Handheld MIRA DS and Tabletop Wasatch Raman Systems

Table 5 summarizes the LODs observed for the various SERS experiments performed with the handheld MIRA DS Advanced Raman system and the tabletop Wasatch Raman setup. Overall, LODs were similar between the two systems. Although the soaking protocol marginally outperformed the droplet protocol for the MIRA DS system, from an ease-of-use standpoint, the droplet protocol is preferred and is highlighted green in the table. While the soaking experiments were performed, the entire P-SERS strip became saturated with liquid, which made handling very difficult. Several strips had to be thrown away, and experiments had to be repeated because of strips tearing or bending in a way that prevented their proper placement in the MIRA SERS attachment for measurement. Our opinion and recommendation moving forward is to use the MIRA DS Advanced system and the SERS attachment with the droplet protocol and the laser raster setting turned on. This is further discussed in the project summary (Section 5).

Table 5. Summary of LODs for Fentanyl Compounds Obtained Using Wasatch Tabletop Raman System and MIRA Handheld Raman System with Droplet and Soaking Protocols

Fentanyl Compound	LOD (M)						
	Wasatch Ag P-SERS Droplet	Wasatch Au P-SERS Droplet	MIRA Droplet, Raster	MIRA Droplet, No Raster	Wasatch 1 min Immersion	MIRA 1 min Immersion, No Raster	MIRA 1 min Immersion, Raster
Sufentanil	1.00×10^{-5}	1.00×10^{-6}	1.00×10^{-6}	1.00×10^{-5}	1.00×10^{-6}	1.00×10^{-6}	1.00×10^{-6}
Alfentanil	1.00×10^{-4}	1.00×10^{-4}	1.00×10^{-5}	1.00×10^{-4}	1.00×10^{-5}	1.00×10^{-4}	1.00×10^{-5}
Fentanyl	1.00×10^{-6}	1.00×10^{-5}	1.00×10^{-7}	1.00×10^{-6}	1.00×10^{-7}	1.00×10^{-7}	1.00×10^{-7}
Benzylfentanyl	1.00×10^{-6}	1.00×10^{-5}	1.00×10^{-7}	1.00×10^{-6}	1.00×10^{-7}	1.00×10^{-7}	1.00×10^{-7}
Remifentanil	1.00×10^{-4}	1.00×10^{-3}	1.00×10^{-4}	1.00×10^{-4}	1.00×10^{-5}	1.00×10^{-5}	1.00×10^{-5}

Note: Green indicates results from preferred droplet protocol.

3.4 Results and Discussion: Thermo H-Kit SERS

In conjunction with the P-SERS experiments, slightly differently protocols were applied to perform measurements using the Thermo H-Kit substrates. The H-kit substrates have a more rigid, silicon background; therefore, measurements were performed using a laboratory-grade WITec Raman chemical imaging microscopy system (WITec Wissenschaftliche Instrumente und Technologie; Ulm, Germany). Brightfield and SEM images of the substrates are shown in Figure 27.

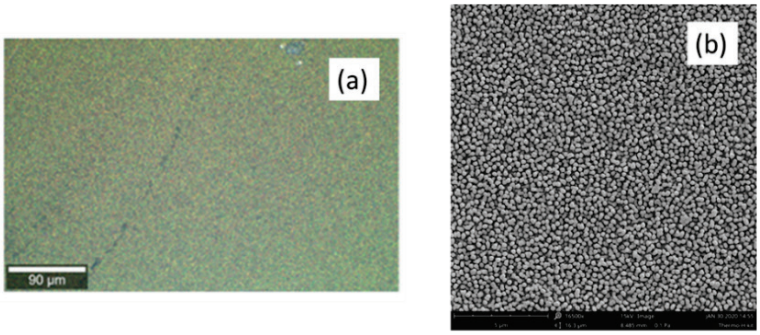

Figure 27. An H-Kit Au nanopillar substrate: (a) brightfield image and (b) SEM image showing greater detail.

For these measurements, a 785 nm excitation laser was used with 1 mW laser power and a 20× microscope objective. A 200 × 200 µm area on the substrates was analyzed. An array of 100 × 100 points was measured with 0.1 s integration time per point (Figure 28). After each spectrum was corrected for cosmic rays and then baselined, the average spectra were calculated for the set of spectra. Because of the tight focusing of the laser beam in this Raman microscope system, there was significant variability in the individual single-pixel Raman spectra. Averaging the spectra over a Raman map resulted in a spectrum that was more representative of the spectrum obtained with a handheld instrument.

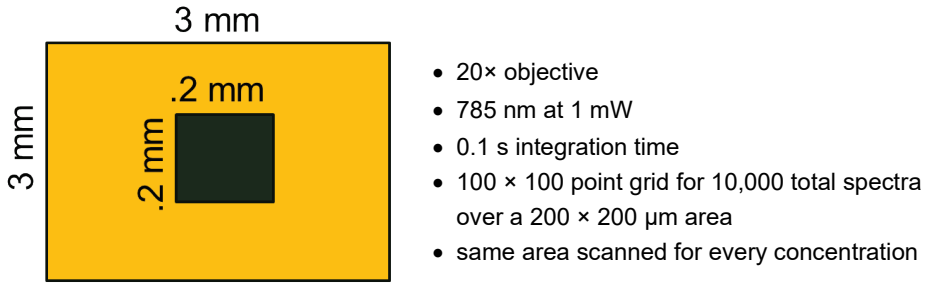

Figure 28. Analysis parameters for measurements of the Thermo H-Kit substrates on the WITec microscope.

For each analyte studied, a series of concentrations ranging from 1.0×10^{-6} through 5.0×10^{-3} M were measured; in addition, a blank solvent measurement was performed. For each analyte, a series of three replicates were measured. At each concentration, the substrate was immersed and gently agitated in a shaker for 10 min. It was then air-dried in a stream of inert gas immediately before the measurement was performed. Results for benzylfentanyl, fentanyl, and remifentanil are shown in Figures 29–31. Sufentanil and alfentanil were also examined but exhibited no useable data points, which is indicative of poor binding between the target analyte and the gold surface. In general, the performance of these Au nanopillar substrates was poorer than that of the Ag paper-based SERS substrates described in Section 3.2. This may be because different metallic elements were used; Ag may have a higher affinity for fentanyls than Au (as shown in Table 5). There is also a structural difference between the two substrates that may impact the overall enhancement. The Thermo H-Kit is a planar substrate in which the nanostructured Au is stationary (in the form of pillars). This means that the analyte interacts with gold only in a certain manner: it adsorbs to the surface. The P-SERS substrate is porous and contains colloidal nanoparticles. Although these nanoparticles are bound to the fibrous material of the filter paper, they can move and interact with the analyte in various ways and then essentially redeposit onto the fibrous material. This can happen over a period of seconds. This additional interaction could be the reason that the P-SERS substrates demonstrate higher enhancements than the Au nanopillar substrates.

Furthermore, as compared to the P-SERS substrates, the spectral responses of the H-Kits are less rich. Even at the highest concentrations, generally, only the largest peak (near 1000 cm^{-1}) is observable, and it is not very distinctive for discriminating between different types of synthetic opioids and other aromatic molecules with isolated phenyl groups.

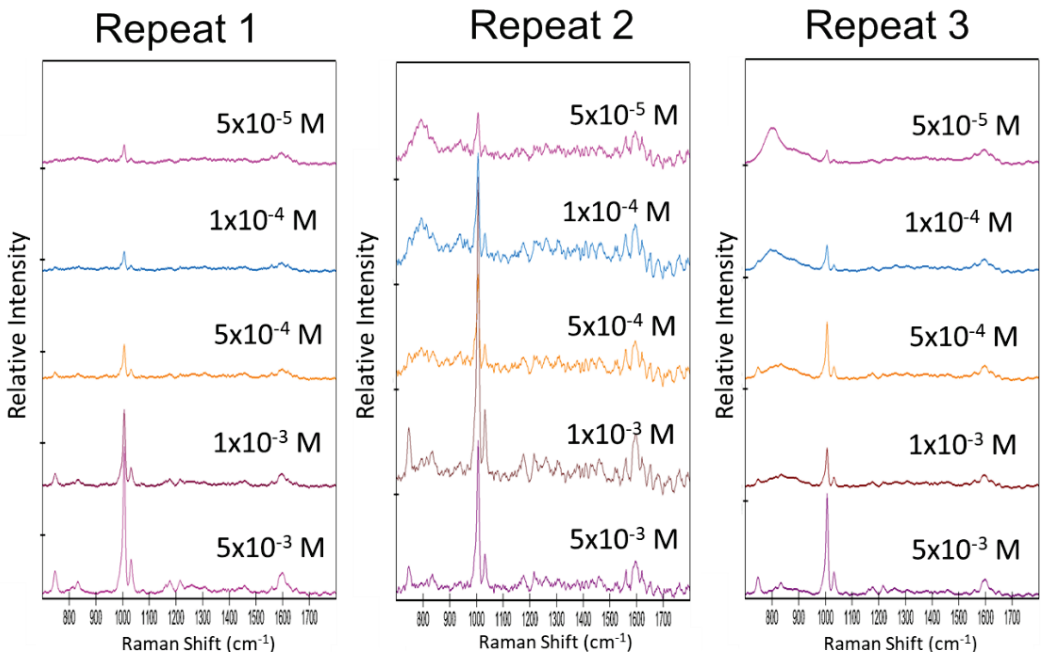

Figure 29. Concentration-dependent SERS spectra of benzylfentanyl on H-Kit substrates. Average spectra are shown.

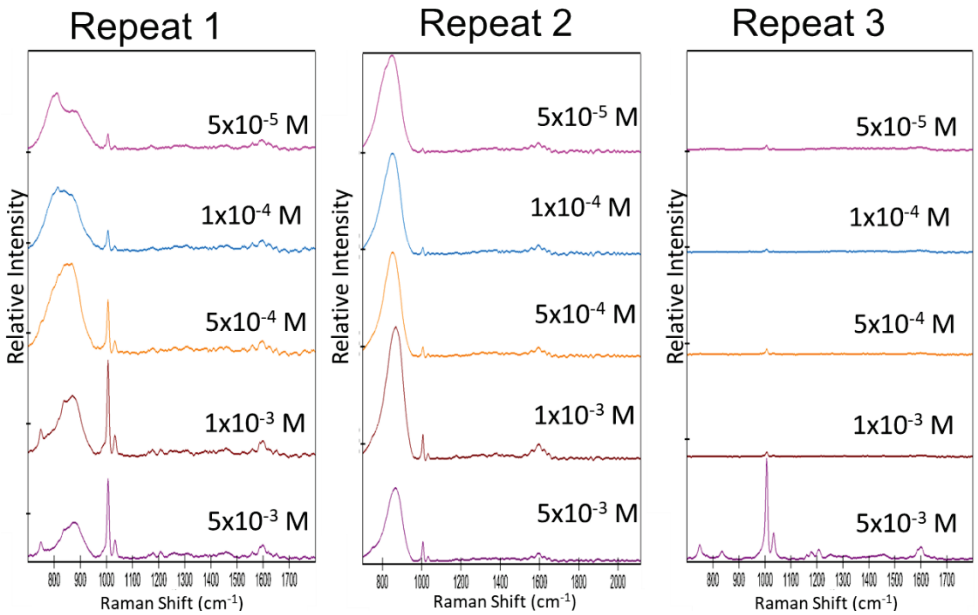

Figure 30. Concentration-dependent SERS spectra of fentanyl on H-Kit substrates. Average spectra are shown.

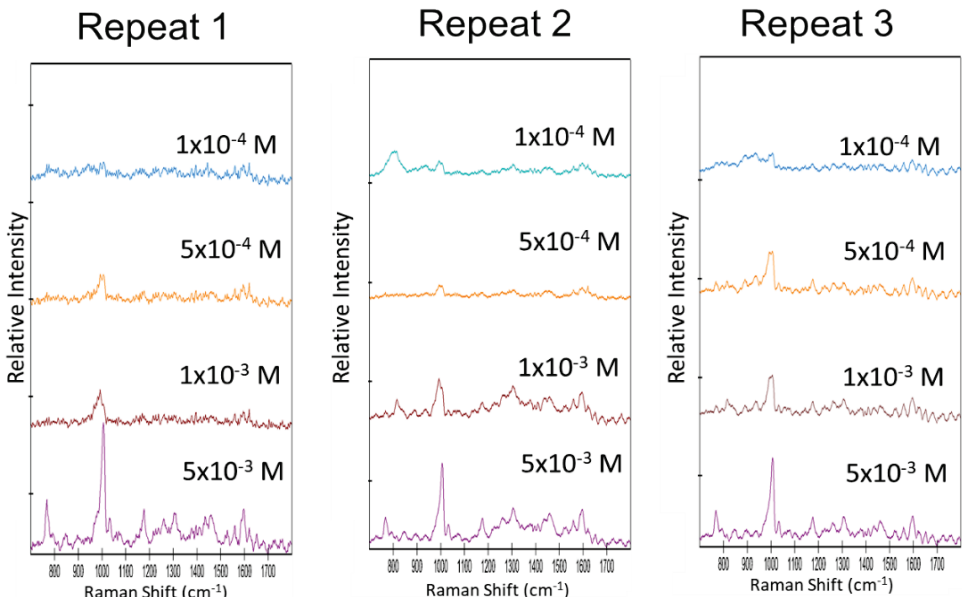

Figure 31. Concentration-dependent SERS spectra of remifentanil on H-Kit substrates. Average spectra are shown.

Overall, the H-Kits exhibited less-than ideal responses when used with the investigated synthetic opioids. They were not further analyzed with the portable systems and were removed from the investigation.

3.5 Orthogonal System P-SERS Measurements

For SERS to be considered as a potential accessory for trace-level analysis of Raman systems, the substrates must be used on various systems (regardless of manufacturing company). Along with work described in Section 3.2 with the P-SERS strips and the MIRA DS system, we analyzed a subset of the prepared opioid samples on a prototype Raman microscopy system.

The Portable Chemical Fingerprint Identification System (P-CFIS) was developed as a next-generation device of the Chemical Fingerprint Identification System concept developed by the DEVCOM CBC Spectroscopy Branch. Developed by Pendar Technologies (Cambridge, MA), the P-CFIS is the first portable Raman microscopy system designed to rapidly ascertain threat chemical information from common surfaces of varying curvature (such as plastics, metals, paper, etc.). An analysis is performed in less than 3 min from a fixed standoff distance of at least 1 in. from the interrogated surface, which may be flat or uneven and chemically heterogeneous. The P-CFIS was originally built specifically for the MIRA DS system. We adapted the P-CFIS to work with the Metrohm Raman P-SERS substrate (Figure 32) to demonstrate a secondary Raman system capable of analyzing a commercial substrate.

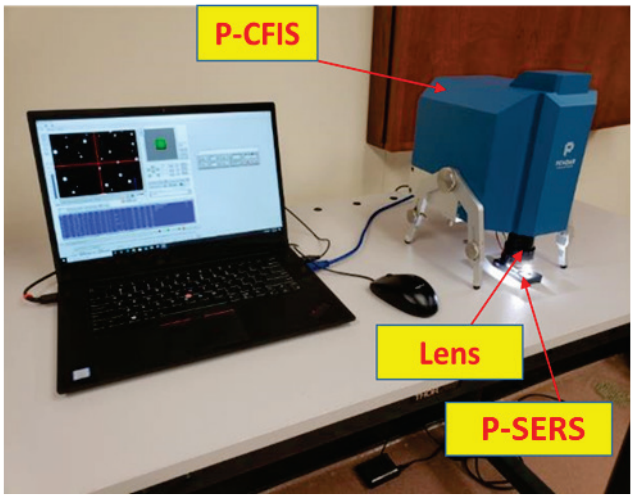

Figure 32. P-CFIS configured to work with P-SERS substrates.

The P-CFIS uses differential Raman equipped with two lasers, 783 and 785 nm. The two lasers acquire individual Raman spectra at each point and then subtract from each other to remove the fluorescence background. The microscopy component is composed of a single lensed architecture; the spot to be interrogated is located with the magnification objective, and Raman acquisition then occurs through the same lens. The illumination of the P-SERS substrate is achieved by dark-field imaging, which tends to "light up" particulates present on the substrate. In the case of the P-SERS strips, the particulates are clusters of aggregated nanoparticles. Figure 33 shows the aggregated nanoparticle on a P-SERS strip exposed to 1.0×10^{-4} M of fentanyl as viewed by the P-CFIS. The system software locates particles of interest autonomously and then targets them for Raman analysis.

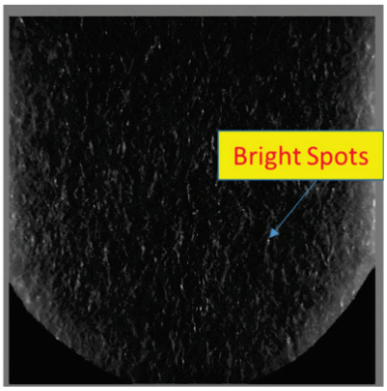

Figure 33. P-CFIS viewing P-SERS strip, targeting particles of interest (white bright spots).

3.5.1 P-CFIS Settings

The P-SERS strip is placed under the microscope, and the operator uses the P-CFIS software to focus the sample. The P-CFIS microscopy software automatically identifies the location of each bright spot using *x*, *y,* and *z* axis coordinates (as shown in Figure 33). The instrument was set to scan a height of 600 µm to achieve optimum focus at each spot. The laser current was set to 300 mA for 783 nm and 306 mA for 785 nm. The integration time for each spectrum was set to 6 s. For each SERS strip, 50 spots were interrogated. At each spot, the two-laser spectra and an image from where the spectra were taken were recorded.

3.5.2 Preparing the SERS Strips

After the P-SERS substrates were analyzed on the MIRA DS system (shown in Figures 22–26), the same strips were then analyzed on the P-CFIS. For each SERS strip, the P-CFIS acquired 50 spectra. The initial focusing and substrate survey took 60 s, 2 s were required for the lens to travel to each spot, and the spectra were acquired in 6 s. Thus, for each SERS strip, the P-CFIS full analysis required approximately 7.5 min and covered an approximately 1 cm^2 area.

3.5.3 SERS Spectral Analysis from P-CFIS

MATLAB code (MathWorks; Natick, MA) was written to auto-collate the spectral data and remove the baseline with a rolling-circle filter. The average spectra per SERS strip was then calculated and displayed with a feather plot of the individual spectra per strip. The peak area of the 1000 cm^{-1} wavenumber Raman stretch for benzene ring breathing mode was determined, and a final correlation analysis was performed with the average spectra obtained using SERS for each of the five opioids at 1×10^{-3} M concentration.

The results for benzylfentanyl and fentanyl (shown in Figure 34) exhibit the characteristic peaks observed in data from both the Wasatch spectrometer and the Raman MIRA DS system. All 50 data points for each concentration were overlaid and demonstrated high repeatability across the P-SERS substrate. Analysis was further performed on the 1000 cm^{-1} band to calculate LODs in a fashion similar to that used to calculate the LODs listed in Table 5.

Table 6 shows the results for all five analytes as well as comparison data collected from the P-SERS strips analyzed by the MIRA DS system. An interesting note: the LODs were quite similar except for an order of magnitude difference for remifentanil.

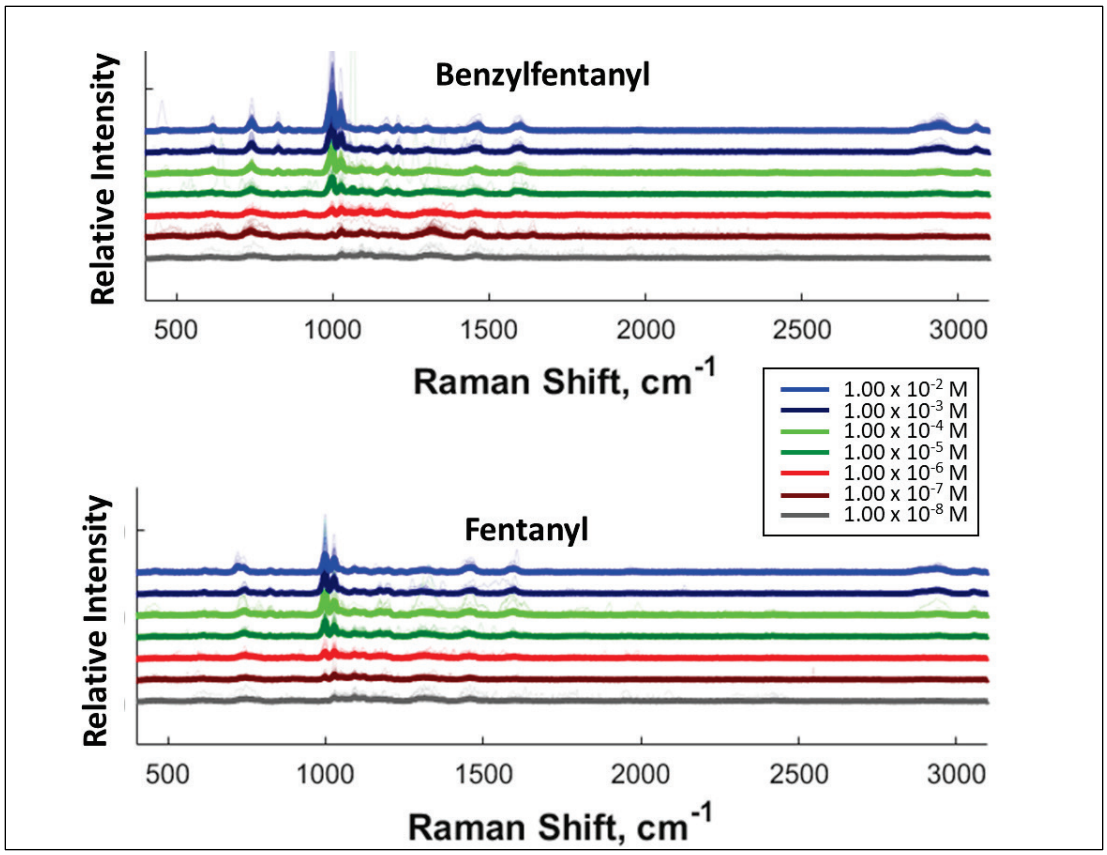

Figure 34. P-CFIS SERS data from P-SERS strips along with LOD calculations.

Table 6. Comparisons of LODs Between P-CFIS and Raman MIRA DS System Using the Same Substrates for Both Analyses

Fentanyl Compound	LOD (M)	
	P-CFIS	MIRA DS*
Sufentanil	1.00×10^{-6}	1.00×10^{-6}
Alfentanil	1.00×10^{-5}	1.00×10^{-5}
Fentanyl	1.00×10^{-7}	1.00×10^{-7}
Benzylfentanyl	1.00×10^{-7}	1.00×10^{-7}
Remifentanil	1.00×10^{-5}	1.00×10^{-5}

*Using soak protocol and raster setting.

The data for the P-CFIS show that the P-SERS strips could be analyzed by a secondary instrument without loss of performance, even after initial measurements were performed on the MIRA DS system. What this potentially demonstrates is the generally noninvasive nature of the technique: once a sample is collected on a P-SERS substrate, measurements can be made by multiple instruments to gain greater confidence in the results.

A SERS summary and path forward are discussed in the project summary (Section 5).

4. MASTER SPECTRUM DEVELOPMENT

As mentioned in the Introduction (Section 1), as new synthetic analogs emerge, it is not always feasible, cost-effective, or timely to acquire a sample of the new compound, add a new element to the library, and disseminate the new library to operators in the field. Instead, it is preferable to have a screening method capable of classifying unknown fentanyl analogs while minimizing false alarms on other benign unknowns. In this section, we explore the possibility of creating a unique, singular synthetic opioid spectrum to demonstrate the ability to classify spectra as fentanyl or non-fentanyl, even if the actual target does not exist in a library database.

4.1 Data Development

All spectra were collected using a Pendar X10 handheld Raman spectrometer. The system uses a unique approach of shifted-excitation Raman difference spectroscopy with two excitation lasers at approximately 825 nm (*3*), which is similar to P-CFIS functionality, as described in Section 3.5. Using the difference of the spectra collected at the two excitation wavelengths, the instrument can reconstruct the traditional Raman spectrum with greatly reduced interference from fluorescence and room lights. This is different from other commercially available instruments that operate with a single laser and use additional algorithms and data processing to mitigate fluorescence and backgrounds. All data analysis was performed using these reconstructed spectra.

Data were divided into two groups. The first group contained long integration scans with high SNRs, which were used to perform the initial analyses and generate the barcode libraries. The second group contained lower SNR data that were collected using the system's automated scan feature. This is the procedure an operator would typically use to collect a spectrum from an unknown material. Using this method, total scan times were typically 1–10 s. The data in this second group were used as validation to assess the real-world performance of the barcode technique.

Each group was further divided into a fentanyl class that contained spectra collected from fentanyl and fentanyl analogs in various free-base or salt forms and a non-fentanyl class that contained all other spectra. A small subset of 28 fentanyl near-neighbors was excluded from analysis. These near-neighbors included spectra from fentanyl precursors and degradation products and non-fentanyl-based synthetic opioids. Because the intended usage is for customs inspection of hazardous material, the included spectra contained a mixture of common

laboratory materials, pharmaceutical compounds, illicit drugs, chemical warfare agents, explosives, and toxic industrial chemicals and materials. After the data were divided, the high-SNR set contained 208 fentanyl spectra and 1796 non-fentanyl spectra. The low-SNR data contained 218 non-fentanyl spectra and 132 individual fentanyl spectra (from 10 different analogs or salts of varying purities and synthetic routes).

4.2 Creation of Average Spectrum

All of the high-SNR fentanyl spectra were averaged to create a single spectrum (Figure 35A). The correlation coefficient between the average spectrum and each high-SNR spectrum was calculated using the following series of equations:

$$\mu_A = \frac{1}{N}\sum_{i=1}^{N} A_i \qquad \mu_B = \frac{1}{N}\sum_{i=1}^{N} B_i \tag{1}$$

$$\sigma_A = \sqrt{\frac{1}{N}\sum_{i=1}^{N} A_i - \mu_A} \qquad \sigma_B = \sqrt{\frac{1}{N}\sum_{i=1}^{N} B_i - \mu_B} \tag{2}$$

$$\mathrm{COV}_{AB} = \frac{1}{N}\sum_{i=1}^{N}(A_i - \mu_A)(B_i - \mu_B) \tag{3}$$

$$\rho_{AB} = \frac{\mathrm{COV}_{AB}}{\sigma_A \sigma_B} \tag{4}$$

where *A* and *B* are the two spectra expressed as *N* point vectors. The mean value (μ) for each spectrum is defined in eq 1. The mean is used to determine the standard deviation (σ) for each spectrum using eq 2. The covariance (COV_{AB}) between the two spectra is given by eq 3. The covariance and standard deviation are used to calculate the correlation coefficient (ρ) using eq 4.

Figure 35B shows the correlation score between the single average fentanyl spectrum and each of the 2004 high-SNR spectra. The correlation scores against the fentanyl compounds are shown in blue, and the scores against non-fentanyl compounds are shown in red. Using these values, it is possible to generate a receiver operating characteristic (ROC) curve shown in Figure 35C to visualize the trade-off between the probability of detection (P_D) and the probability of false alarm (P_{FA}). The optimum point to maximize P_D while minimizing P_{FA} resulted in a P_D of 93% and a P_{FA} of 11%. Comparing the same average spectrum to the low-SNR data gives comparable results with a P_D of 94.7% and a P_{FA} of 7.3%.

Because certain fentanyl analogs have similar changes to their functional groups, it was expected that there would be spectrally similar subclasses. To exploit this and improve performance, more than one average spectrum was explored using *k*-means clustering to automatically group and average like spectra. Figure 35C shows that as the number of spectral clusters was increased, the P_D improved, while the P_{FA} was reduced. This result is not surprising; however, even with a large cluster, the false-alarm rate remained higher than desired (approximately 5% with 40 clusters). Additionally, use of a large number of these clustered average spectra may not be robust against emerging fentanyl analogs or offer a significant benefit over the traditional method of including each fentanyl analog in the library as its own entry. To overcome these limitations, a barcode method was investigated.

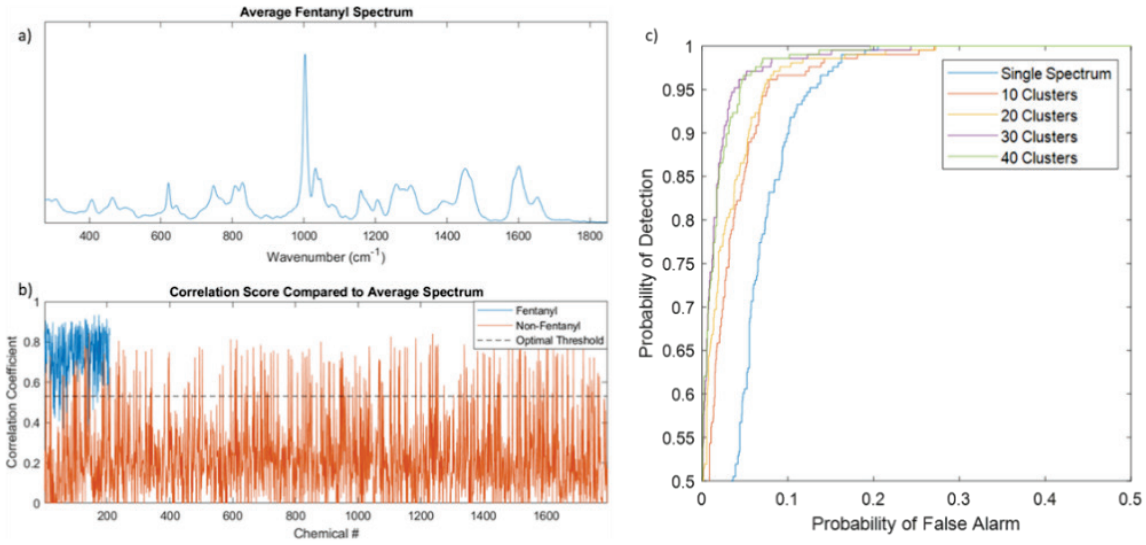

Figure 35. (a) Average of all high-SNR fentanyl spectra. (b) Correlation coefficients between the average fentanyl spectrum and all 208 fentanyl spectra (blue) and 1796 non-fentanyl spectra (red). (c) ROC curve showing the P_D and P_{FA} trade-off that occurs when comparing the high-SNR spectra to different cluster sizes of average spectra.

4.3 Creation of Barcode Spectrum

Creating spectral barcodes is a method of converting continuous Raman peak intensities into binary values that uniquely identify key spectral features. Four different barcoding methods were examined in this effort.

The first was intensity thresholding. In this technique, a percentage threshold is set between the maximum and minimum intensities of the spectrum. Intensity values above the threshold are set to 1, and intensities below threshold are set to zero.

The second method was area thresholding. In this technique, the total area under the spectrum is calculated. An intensity threshold is again used, but the threshold value is set to ensure that a set percentage of the spectral area is above threshold (and set to 1), and the remainder of the below-threshold intensities are set to zero.

The third and fourth methods are based on the first and second derivatives of the spectra, respectively. An example of the barcoding process is shown in Figure 36. The original spectrum is shown in Figure 36a; an arbitrary threshold is shown as the horizontal red dashed line. Figure 36b shows the resulting barcode, where all intensity values above the threshold are set to 1, and all remaining values are set to zero.

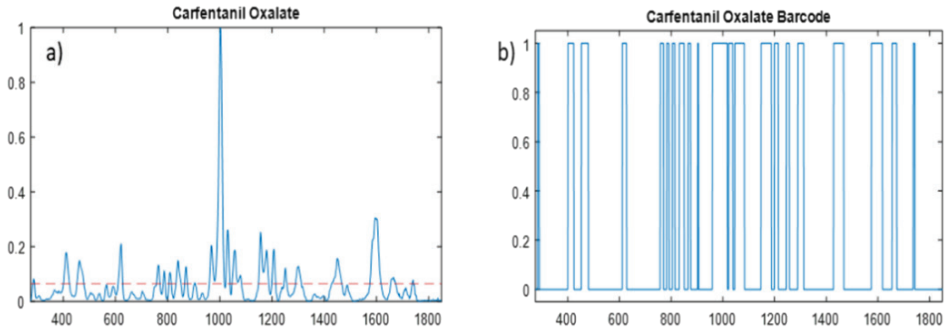

Figure 36. Barcoding example displaying the intensity threshold method showing (a) Raman spectrum of carfentanil oxalate and (b) corresponding carfentanil oxalate barcode spectrum. Threshold was set at red dashed line.

4.4 Data Analysis

All 2004 high-SNR spectra were barcoded. The barcodes of the 208 fentanyl spectra and the 1796 non-fentanyl spectra were then averaged (Figure 37). These averaged barcodes show which spectral features were more or less common in the two classes. Values closer to 1 (e.g., 1000 cm^{-1} for fentanyl-related compounds) indicate that above-threshold spectral features were present in nearly 100% of the spectra. Likewise, values closer to zero indicate that there were few above-threshold spectral features at a given Raman shift. It should be noted that Figures 36–38 were all generated using intensity thresholding. The different barcoding methods resulted in different intermediate results; however, the same procedure was followed with all barcoding techniques.

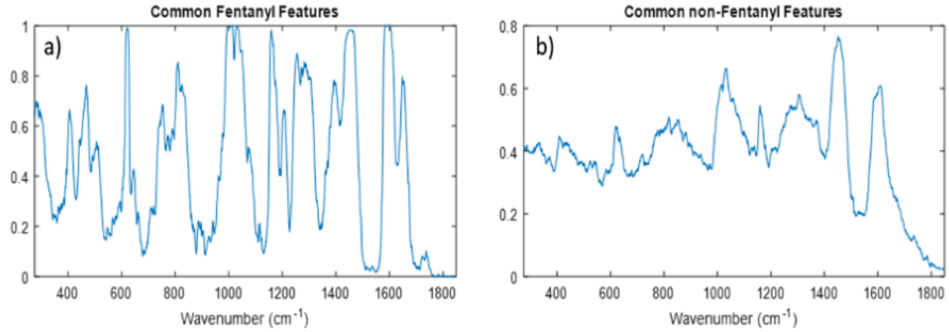

Figure 37. Averages of the barcoded spectra for (a) fentanyl-related compounds and (b) non-fentanyl-related compounds.

The differences between the feature plots from Figure 37 were calculated and are shown in Figure 38a. Values greater than zero indicate barcode features that are more likely to be fentanyl, and values less than zero indicate features that are more likely to be non-fentanyl. The farther the value is from zero, the more likely that the given feature is related to the given class. To take advantage of this relationship, the absolute value of the difference features (Figure 38b) was used to give more weight to these regions. This was done using the weighted correlation coefficient defined in eqs 5–8.

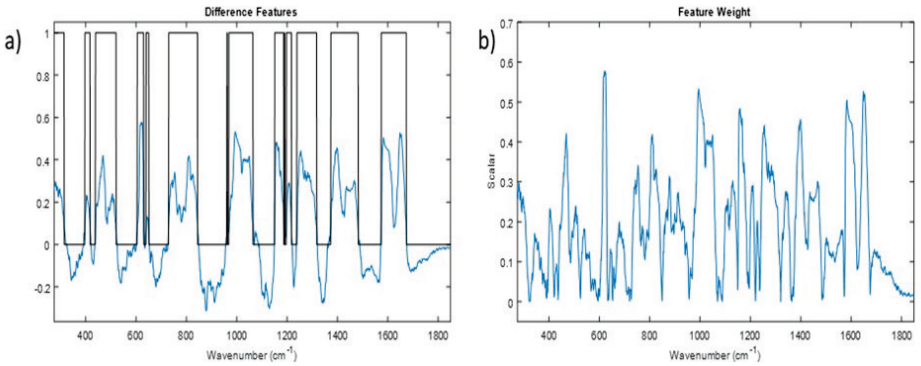

Figure 38. (a) Difference between the common fentanyl barcode features and common non-fentanyl barcode features (blue) and the library barcode (black). (b) Absolute value of the difference features used as weight when calculating the weighted correlation.

$$\mu_A^w = \frac{\sum_{i=1}^{N} w_i A_i}{\sum_{i=1}^{N} w_i} \qquad \mu_B^w = \frac{\sum_{i=1}^{N} w_i B_i}{\sum_{i=1}^{N} w_i} \tag{5}$$

$$\sigma_A^w = \sqrt{\sum_{i=1}^{N} w_i (A_i - \mu_A^w)} \qquad \sigma_B^w = \sqrt{\sum_{i=1}^{N} w_i (B_i - \mu_B^w)} \tag{6}$$

$$\mathrm{COV}_{AB}^w = \sum_{i=1}^{N} w_i (A_i - \mu_A^w)(B_i - \mu_B^w) \tag{7}$$

$$\rho_{AB}^w = \frac{\mathrm{COV}_{AB}^w}{\sigma_A^w \sigma_B^w} \tag{8}$$

The weighted correlation coefficient calculation is similar to the traditional Pearson correlation coefficient that is defined in eqs 1–4, except each point of the spectrum is multiplied by a scalar value defined by the weight vector (w), as shown in Figure 39b. Again, A and B are the two spectra expressed as N-point vectors. The weighted mean value (μw) for each spectrum is defined in eq 5. The weighted mean was used to determine the weighted standard deviation (σw) for each spectrum using eq 6. The weighted covariance (COV_{AB}^{w}) between the two spectra is given by eq 7. The weighted covariance and standard deviation were used to calculate the weighted correlation coefficient (ρw) using eq 8. The weighted correlation was used to calculate the correlation coefficient for all comparisons between barcodes, and the traditional correlation calculation was used to compare between Raman spectra.

The weighted correlation coefficient was calculated between the library barcode and the barcodes generated from the 2004 high-SNR spectra, and the results are shown in Figure 39a. The fentanyl and non-fentanyl classes show better separation with use of the barcode method rather than the average spectrum, which consequently results in a more optimal P_D–P_{FA} trade-off, as shown in the ROC curve in Figure 39b. The optimal P_D–P_{FA} (which maximizes the P_D and minimizes the P_{FA}; closest to the upper-left corner of the ROC curve) for the intensity-thresholded barcode technique improved as compared to the average spectrum technique: the P_D increased from 93.3 to 97.6% while the P_{FA} decreased from 11.1 to 1.5%.

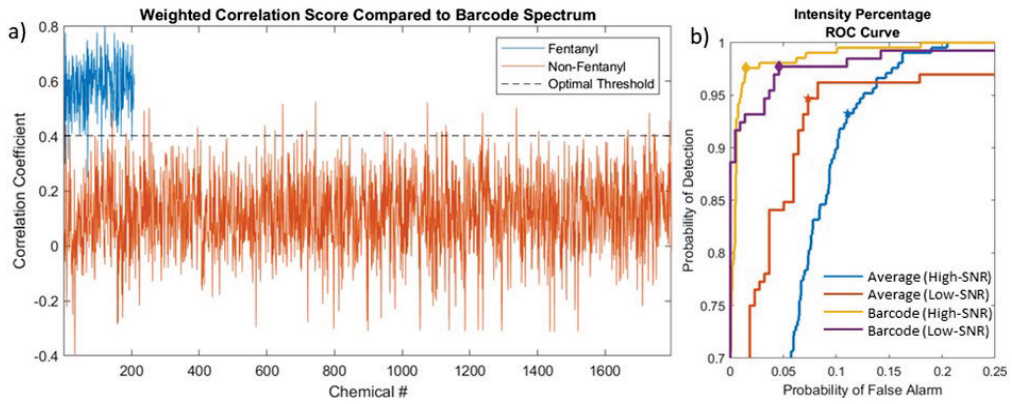

Figure 39. (a) Weighted correlation coefficients between the fentanyl library barcode and all 208 fentanyl barcodes (blue) and 1796 non-fentanyl barcodes (red) generated using intensity thresholding. (b) ROC curve showing the PD and PFA trade-off of both the barcode technique (yellow and purple) and single average spectrum (blue and red). Note: The high-SNR average spectrum was the same as the single spectrum result shown in Figure 36a.

To apply the same procedure to the low-SNR spectra, an 11-point-mean filter was applied to the spectra prior to barcoding. All low-SNR barcoding analyses were performed against library barcodes that were generated from the high-SNR spectra. Figure 40 shows the barcode representation of all the low-SNR spectra defined using the four different barcode methods. At the top is the barcode library. The section between the red lines shows the barcodes for the fentanyl compounds, and below them are the barcodes for the non-fentanyl chemicals. ROC curves were generated for each barcoding method to determine the optimal P_D and P_{FA} for the high- and low-SNR data (Table 7). Generally, the performance of the intensity thresholding, area thresholding, and first derivative methods provided comparable results; however, the intensity threshold method had the lowest P_{FA} against the high-SNR data.

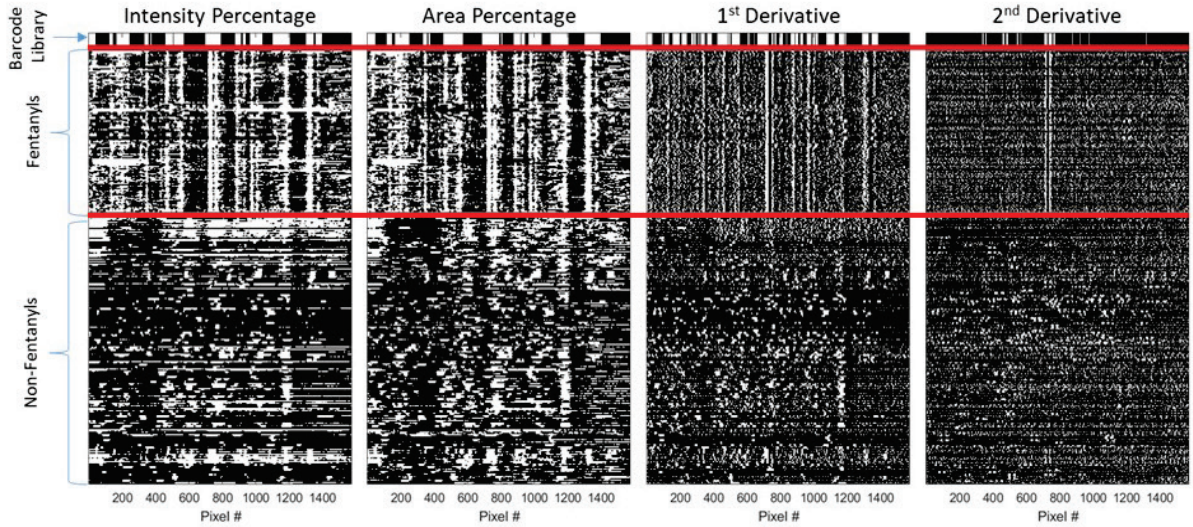

Figure 40. Barcode representations of all low-SNR spectra using the four barcoding techniques. The library barcodes generated by using the high-SNR data are shown at the top, the fentanyl barcodes are shown between the red lines, and beneath them are the non-fentanyl barcodes.

Table 7. Optimized P_D and P_{FA} for Each Classification Method

Method	High SNR				Low SNR			
	P_D		P_{FA}		P_D		P_{FA}	
Average spectrum	194	93.3%	199	11.1%	125	94.7%	16	7.3%
Intensity threshold	203	97.6%	26	1.4%	129	97.7%	10	4.6%
Area threshold	203	97.6%	49	2.7%	126	95.5%	10	4.6%
First derivative	202	97.1%	98	5.5%	127	96.2%	10	4.6%
Second derivative	196	94.2%	215	12.0%	123	93.2%	22	10.1%

Although the ability to discriminate between the two classes results in similar P_D and P_{FA} values for the high- and low-SNR data, it should be noted that the specific threshold for obtaining these results is different. Figure 41 shows the library and the high- and low-SNR barcodes for all of the fentanyl and non-fentanyl compounds, along with the weighted correlation coefficient for each barcode comparison. The detection threshold to distinguish the high-SNR data is larger than the threshold for the low-SNR data.

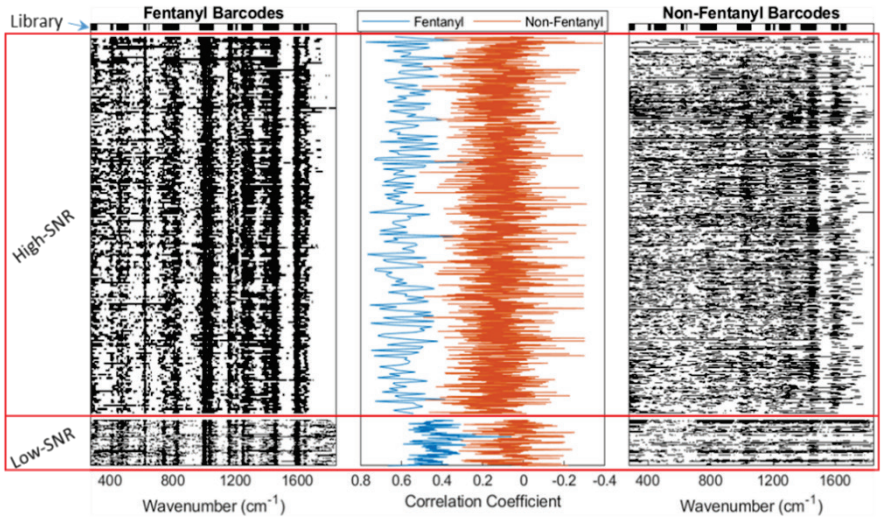

Figure 41. Comparison of library, high-SNR, and low-SNR barcodes for fentanyl compounds (left) and non-fentanyl compounds (right). The weighted correlation coefficient for each spectrum is also shown (middle).

5. PROJECT SUMMARY

The ability to provide rapid, reliable, trace detection of chemical, biological, and explosive threats in multiple application spaces is still a critical need on the battlefield and for defense personnel. The potential advantages that SERS provides along with the inclusion of a normal Raman master spectrum could impact new military-relevant sensing areas including post-decontamination scenarios; trace detection of chemical, biological and explosive materials; and even classification of an unknown in the environment. In this study, we have shown SERS to detect low concentrations of synthetic opioids by several orders of magnitude beyond the current

detection levels of normal Raman spectroscopy and the systematic development of a single unique spectrum, in a traditional spectrum form or a transcribed barcode, in order to make a first-line classification of a potential unknown, new analog of a synthetic opioid. Although none of the data are conclusive, this work shows the potential and the need for the continued exploration and investigation of these types of techniques.

The investigated P-SERS strips exhibited LODs as low as 1×10^{-7} M (fentanyl, benzylfentanyl), which roughly equates to nanogram per milliliter levels. This would be on par with needed detection limits of adulterated opioids in the 1–10% weight/weight levels observed in the field. This also potentially bridges the gap of normal Raman handheld detectors that typically degrade in performance at 10% purity levels. Moving forward, the burden of ensuring a proper interaction with the SERS substrate still needs to be developed, along with use-case scenarios of where SERS-based techniques would have the greatest impact. We observed differences between the rigid planar substrate (Thermo H-Kit) and the colloidal-based P-SERS strips, which is an example of this different analyte-to-substrate interaction. The P-SERS strips consistently performed better. This was potentially because of the ability of the colloids to displace from the fibrous substrate materials, thereby allowing greater interaction with the analyte before analysis.

For use-case scenarios, currently fielded trace opioid detection techniques, such as colorimetric analysis, comprise an area to investigate for potential impact. Although they are sensitive and easy to use, colorimetric kits have inherent shortcomings: the reading of color changes by users is subjective, and multiple types of kits are required to detect a host of different materials (i.e., kits for opioids, tetrahydrocannabinol, explosives, etc.). A SERS-based technique that uses a broad enhancing substrate, similar to the P-SERS strips, in conjunction with a handheld Raman device, could negate the need to carry around multiple colorimetric kits. Furthermore, with the orthogonal measurements between the MIRA DS and the P-CFIS systems demonstrated, there is potential that an initial analysis could be performed nondestructively in the field. This would allow for the samples to be further analyzed by conformational technologies at a later time. More research needs to be performed to tease out these potential advantages and to better understand the limitations associated with highly complex or adulterated materials.

The main focus of the SERS research was the low-level detection of opioids. One item that was not investigated but has been theorized is the ability of SERS to also enable rapid biological detection. This would truly augment portable Raman spectroscopy by enabling chemical, biological, and trace-level detection from a single instrument in the field.

This demonstration of the unique Raman spectrum using an average and barcode approach provides a possible solution to the problems of novel threat compounds going undetected and the lag time needed to update libraries with newly discovered substances.

Future research in this area should focus on porting and testing developed master spectral data to other Raman systems, as well as general incorporation of data into spectral libraries. A challenge we were unable to address in this work was how best to insert this type of information (spectrum) into multiple handheld Raman systems. The problem stems from each system typically having variable spectral resolution and coverage requirements (including,

possibly, different operating wavelengths) inherent to the internal spectrometers. However, we believe these are challenges that can be overcome with additional data processing and deconvolution techniques that would enable matching of the spectral characteristics to the unique instrument characteristics.

If a proper class-based master spectrum can be constructed for the various chemical threats, such as opioids in this case, but extended to chemical warfare agents and explosive-type materials, then it is possible that Raman could be broadly used as a rapid field detection methodology to provide actionable information on unknown materials. This would allow users to make early decisions on next best steps for mitigating threats.

LITERATURE CITED

1. *2020 National Drug Threat Assessment, Strategic Intelligence Section*; DEA-DCT-DIR-008-21; U.S. Department of Justice, Drug Enforcement Administration: Washington DC, March 2021; https://www.dea.gov/sites/default/files/2021-02/DIR-008-21%202020%20National%20Drug%20Threat%20Assessment_WEB.pdf (accessed 1 September 2022).

2. Temporary Listing of Substances Subject to Emergency Scheduling. Schedules of Controlled Substances. *Code of Federal Regulations*; Title 21, Chapter II, Part 1308, Section 1308.11(h), 2022; https://www.ecfr.gov/current/title-21/chapter-II/part-1308/subject-group-ECFRf62f8e189108c4d/section-1308.11 (accessed 1 September 2022).

3. Blanchard, R.; Vakhshoori, D. Standoff Detection of Chemicals Using Infrared Hyperspectral Imaging and Raman Spectroscopy. In *Proceedings Volume 11416: Chemical, Biological, Radiological, Nuclear, and Explosives (CBRNE) Sensing XXI.* SPIE Defense + Commercial Sensing, 24 April 2020. Society of Photo-Optical Instrumentation Engineers (SPIE): Bellingham, WA, 2020; https://doi.org/10.1117/12.2558806 (accessed 1 September 2022).

Blank

ACRONYMS AND ABBREVIATIONS

DEA	U.S. Drug Enforcement Agency
DEVCOM CBC	U.S. Army Combat Capabilities Development Command Chemical Biological Center
EtOH	ethanol
IPS	Innovative Photonics Solution
IUA	intelligent universal attachment
LC	liquid chromatography
LOD	limit of detection
MIRA	Metrohm Instant Raman Analyzer
MS	mass spectrometry
NMR	nuclear magnetic resonance
P-CFIS	Portable Chemical Fingerprint Identification System
P_D	probability of detection
P_{FA}	probability of false alarm
P-SERS	printed-surface enhanced Raman spectroscopy
ROC	receiver operating characteristic
SEM	scanning electron microscopy
SERS	surface-enhanced Raman spectroscopy
SNR	signal-to-noise ratio
TP	thiophenol

DISTRIBUTION LIST

The following individuals and organizations were provided with one electronic version of this report:

U.S. Army Combat Capabilities Development Command Chemical Biological Center (DEVCOM CBC)
FCDD-CBR-IS
ATTN: Guicheteau, J.
Vanderbeek, R.

Department of Homeland Security
Office of Mission Capability and Support
ATTN: Anderson, R.

DEVCOM CBC Technical Library
FCDD-CBR-L
ATTN: Foppiano, S.
Stein, J.

Defense Technical Information Center
ATTN: DTIC OA

U.S. ARMY COMBAT CAPABILITIES DEVELOPMENT COMMAND
CHEMICAL BIOLOGICAL CENTER